Design of antibacterial apatitic composite cement loaded with Ciprofloxacin: Investigations on the physicochemical Properties, release Kinetics, and antibacterial activity

Hanaa Mabroum, Hamza Elbaza, Hicham Ben Youcef, Hassane Oudadesse, Hassan Noukrati, Allal Barroug

▶ **To cite this version:**

Hanaa Mabroum, Hamza Elbaza, Hicham Ben Youcef, Hassane Oudadesse, Hassan Noukrati, et al.. Design of antibacterial apatitic composite cement loaded with Ciprofloxacin: Investigations on the physicochemical Properties, release Kinetics, and antibacterial activity. International Journal of Pharmaceutics, 2023, 637, pp.122861. 10.1016/j.ijpharm.2023.122861 . hal-04061340

HAL Id: hal-04061340
https://hal.science/hal-04061340

Submitted on 16 May 2023

HAL is a multi-disciplinary open access archive for the deposit and dissemination of scientific research documents, whether they are published or not. The documents may come from teaching and research institutions in France or abroad, or from public or private research centers.

L'archive ouverte pluridisciplinaire **HAL**, est destinée au dépôt et à la diffusion de documents scientifiques de niveau recherche, publiés ou non, émanant des établissements d'enseignement et de recherche français ou étrangers, des laboratoires publics ou privés.

Distributed under a Creative Commons Attribution - NonCommercial 4.0 International License

Journal Pre-proofs

Design of Antibacterial Apatitic Composite Cement Loaded with Ciprofloxacin: Investigations on the Physicochemical Properties, Release Kinetics, and Antibacterial Activity

Hanaa Mabroum [a,b], Hamza El Baza [b], Hicham Ben Youcef [c], Hassane Oudadesse [d], Hassan Noukrati [b*], Allal Barroug [a,b]

[a] *Cadi Ayyad University, Faculty of Sciences Semlalia, 2390, 40000, Marrakech, Morocco*

[b] *Institute of Biological Sciences, ISSB, Faculty of medical sciences (FMS), Mohammed VI Polytechnic University (UM6P), Ben Guerir, 43150, Morocco,*

[c] *High Throughput Multidisciplinary Research Laboratory (HTMR), Mohammed VI Polytechnic University (UM6P), Ben Guerir, 43150, Morocco,*

[d] *Univ Rennes, CNRS, ISCR-UMR 6226, F-35000 Rennes, France*

Abstract

This work aims to develop an injectable and antibacterial composite cement for bone substitution and prevention/treatment of bone infections. This cement is composed of calcium phosphate, calcium carbonate, bioactive glass, sodium alginate, and ciprofloxacin. The effect of ciprofloxacin on the microstructure, chemical composition, setting properties, cohesion, injectability, and compressive strength was investigated. The in vitro drug release kinetics and the antibacterial activity of ciprofloxacin-loaded composites against staphylococcus aureus and Escherichia coli pathogens were investigated.

XRD and FTIR analysis demonstrated that the formulated cements are composed of a nanocrystalline carbonated apatite analogous to the mineral part of the bone. The evaluation of the composite cement's properties revealed that the incorporation of 3 and 9 wt% of ciprofloxacin affects the microstructural and physicochemical properties of the cement, resulting in a prolonged setting time, and a slight decrease in injectability and compressive strength.

The in vitro drug release study revealed sustained release profiles over 18 days. The amounts of ciprofloxacin released per day (0.2 –15.2 mg/L) depend on the cement composition and the amount of ciprofloxacin incorporated. The antibacterial activity of ciprofloxacin-loaded cement

composites attested to their effectiveness to inhibit the growth of Staphylococcus aureus and Escherichia coli.

Keywords: Calcium phosphate cement, Composites, Ciprofloxacin, Release kinetic, Antibacterial activity.

Journal Pre-proofs

1. Introduction

Because of the harmful effects of bacterial infections on human and animal health, scientists have been focusing for decades to develop antibacterial materials. Several antimicrobial agents have been discovered by scientists, including antibiotics (Bazán Henostroza et al., 2022; Ginebra et al., 2012a; Wang et al., 2021), peptides (Kai et al., 2018), free halogens (Li et al., 2016), metal oxides (Pachaiappan et al., 2021; Yang et al., 2019), graphene oxide, quaternary ammonium salts, and N-halamines (Bu et al., 2021). Despite the efforts of researchers to find new antibacterial agents, antibiotics remain to date the most commonly prescribed agents by clinicians for patients with infectious diseases.

Osteomyelitis is a common inflammatory bone disease that frequently results in necrosis and bone tissue damage and can be caused by polymicrobial infection (Beck-Broichsitter et al., 2015). The main bacteria responsible for bone infections are Staphylococcus aureus (S. Aureus) and Escherichia coli (E. Coli) (Jenkins et al., 2015). The most effective treatment of bone infections is only achieved when the local antibiotic concentration remains above the minimum inhibitory concentration for an extended period, which often could not be provided by the conventional route of antibiotic administration (Rao et al., 2011; Wu et al., 2019). Hence, the potential of local antibiotic therapy which is a novel approach that allows relatively high concentrations of antibiotics ensures an easy access of the drug into the diseased site by inhibiting bacterial growth (Nadig et al., 2020; Nandi et al., 2016). Therefore, materials that function as bone substitutes and carriers for local drug delivery to the site of a defect are in high demand in orthopedics.

Calcium phosphate cements (CPC) have proven to be efficient bone substitutes in different applications thanks to their interesting biological properties, and similarity to the bone mineral (Yousefi, 2019). Due to their low-setting temperature, these materials can incorporate various drugs, without denaturation and losing their therapeutic activity (Ginebra and Montufar, 2019). This property makes CPC-based materials very appealing candidates for the administration of various drugs for the treatment of bone diseases (Fosca et al., 2022).

The incorporation of these therapeutic agents affects the physicochemical features of calcium phosphate cements. Generally, the incorporation of bioactive molecules impacted the composition, morphology, reaction and setting time, injectability, and cohesion as well as mechanical strength (Canal et al., 2013a; Ginebra et al., 2012b; Pastorino et al., 2015a).

The release kinetics of active ingredients from CPCs depends on several parameters, namely: the microstructure (percentage of porosity, pore size, and tortuosity) and composition of the

cements, the solubility of the active ingredient, and possibly physicochemical factors that condition the degradation of the material and also influence the bonds at the interface between the material and the therapeutic agent (Fosca et al., 2022).

The release of the active ingredient can be governed by diffusion, erosion, and/or dissolution mechanisms. But the release can also be related to several mechanisms at the same time. In order to give a good interpretation of the release data, semi-empirical and theoretical models used in pharmacokinetics (Mircioiu et al., 2019) have been successfully applied as tools for the qualitative and quantitative evaluation of drug release from CPCs.

CPCs have been associated with therapeutic agents such as osteoporotic agents for the treatment of osteoporosis (Jindong et al., 2010; Verron et al., 2014), anti-inflammatory agents such as ibuprofen (Alexopoulou et al., 2016), antibiotics for the treatment of bone infections, such as sodium fusidate (Noukrati et al., 2016), tetracycline (Ratier et al., 2004), vancomycin, and ciprofloxacin (Ait Said et al., 2021; Ghosh et al., 2016).

Ciprofloxacin ($C_{17}H_{18}FN_3O_3$), is one of the broad-spectrum carboxyfluoroquinolone antimicrobial agents with excellent activity against both gram-positive and gram-negative bacteria (Raj et al., 2013). The use of locally delivered ciprofloxacin as an antibacterial agent could be an alternative treatment to conventional therapy. The incorporation of ciprofloxacin into biomaterials for the local treatment of bone infection has been the subject of several scientific studies, but only a few studies have focused on the incorporation of this antibiotic into CPCs (Ghosh et al., 2016; Mabrouk et al., 2013; Uskoković, 2019).

The current study focuses on the design of a drug delivery system for the treatment of bone infection. We incorporated ciprofloxacin antibiotic into a mixed cement based on calcium phosphate, calcium carbonate, bioactive glass, and sodium alginate. We first investigated the effect of incorporating the ciprofloxacin on the setting, rheological, and mechanical properties of the prepared composite.

The influence of the antibiotic dose and cement state on release kinetics is further investigated and then, the antibacterial effectiveness was assessed for ciprofloxacin-loaded cements against *Staphylococcus aureus* (*S. aureus*) and *Escherichia Coli* (*E. Coli*) strains, bacteria responsible for bone infections.

Journal Pre-proofs

2. Materials & Methods

2.1. Formulation of reference and composite cements loaded ciprofloxacin

The reactive powders used for formulating the examined cements were explored in our previous paper and consisted of brushite (dicalcium phosphate dihydrate, DCPD, $CaHPO_4.2H_2O$), calcium carbonate (vaterite, $CaCO_3$), and, 46S6 bioactive glass (BG) composed of SiO_2 (46 wt%), Na_2O (24 wt%), CaO (24 wt%), and P_2O_5 (6 wt%) (Mabroum et al., 2021).

The reference composite cement CPC-BG-Alg-NaP, named (RCC) was formulated by combining 25% wt of BG (46S6) powder with an equimassic mixture of $CaCO_3$ and DCPD. These reactive powders were then mixed with a gel composed of sodium alginate solubilized in Na_2HPO_4 solution (0.25M), at an L/P ratio of 0.7.

The formulation of the ciprofloxacin-loaded reference composite cement (RCC-Cip3 and RCC-Cip9) was performed by homogeneously mixing two doses (3 or 9% by mass) of the ciprofloxacin powder (from Sigma–Aldrich (>98% purity) with the reactive powders. The resulting pastes were placed immediately after preparation in a polyethylene tube at a physiological temperature (37°C) and 100 % relative humidity for 48 hours. The hardened and dried cements were characterized after 2 days of maturation and 5 days of drying at 37 °C. The composition of the prepared composite cements is shown in table 1.

Table 1. Composition of formulated cements.

Cements	Powder phase				Liquid phase	L/P
	$CaCO_3$ (wt %)	DCPD (wt %)	BG (wt%)	Cip (*wt %)		
RCC	37.5	37.5	25	0	5 wt % Alg in Na_2HPO_4 (0.25M)	0.7
RCC-Cip3	36	36	25	3		
RCC-Cip9	33	33	25	9		

2.2. Physicochemical characterization of ciprofloxacin-loaded cement

The effect of the incorporation of ciprofloxacin on the properties of the reference composite cement (RCC) was assessed using complementary techniques. The phase identification of the prepared materials was assessed by X-ray diffraction (XRD) using Rikagu D/Max-IIIB apparatus (CuKα source) at ambient temperature. XRD data were collected from 10 to 70° (2θ) with a precision of 0.02° per step and a scan speed of $2.min^{-1}$. Transmission Fourier Transform Infrared spectroscopy (FTIR) was used in order to identify the chemical composition of the formulated cements. The IR spectra were acquired on a Nicolet 5700 spectrometer on powder

samples that were embedded in KBr pellets. The spectra were collected between 4000 cm^{-1} and 400 cm^{-1} with a resolution of 2 cm^{-1}.

The morphology was evaluated through Scanning Electron Microscopy (SEM) using TESCAN VEGA3 apparatus coupled to an EDX spectrometer. All specimens were coated with a thin conductive carbon layer for 30 s using (carbonA coater).

Mercury Intrusion Porosity (MIP) measurements were carried out by a mercury porosimeter (Micromeritics AutoPore IV 9500 V1.09).

2.3. Evaluation of the properties of the ciprofloxacin-loaded cement

2.3.1. Setting properties

The influence of the incorporation of ciprofloxacin on the setting properties of the reference composite cement (RCC) was investigated by examining the kinetics of the setting reaction and setting time. The prepared pastes were incubated for different periods of time ranging from 2 to 48h (2, 4, 6, 24, and 48 hours) in 100% relative humidity conditions at 37 C° and then freeze-dried to inhibit the setting reaction of the cements. To compare the setting reaction kinetics of prepared materials, The dried samples were analyzed by XRD and a peak area ratio of apatite/vaterite (A_{Ap}/A_{Vat}) was calculated as an indicator of apatite formation, using origin software. The terms A_{Ap} and A_{Vat} refer to XRD peak regions at 26° and 25.2° (2θ degree) of the precipitated apatite and vaterite, respectively. Peak area ratios for apatite and vaterite were determined using the most distinct peaks (at 26° and 25.2°) as the most intense peaks are overlapped.

The specimen's initial and final setting times were measured using a Gillmore testing device in accordance with the ASTM C266-89 standard.

2.3.2. Cohesion and Injectability testing

The cohesion test of the prepared cement was performed to assess the ability of the cement pastes to harden in solution without disintegrating. For this purpose, the cement pastes were injected directly after their preparation (3 minutes) in the phosphate buffer solution (PBS). The cohesion was evaluated visually by photographing samples after 5 minutes and 24 hours of injection.

Injectability was evaluated by extruding cement pastes (2 g) using an apparatus applying a constant force of 12N, equipped with a disposable syringe (5 mL capacity and a 2 mm diameter opening nozzle). Injectability values (I%) were determined according to equation (Eq 1):

Journal Pre-proofs

$$I(\%) = \frac{w_{injected}}{w_{initial}} * 100 \qquad \text{(Eq 1)}$$

where $w_{initial}$ and $w_{injected}$ are respectively, the weights of the paste initially introduced in the syringe and the paste injected, and I is the injectability. All values were the average of three performed tests for each sample.

2.3.3. Compressive strength

The mechanical properties tests (compressive strength) of the prepared reference and composite cements were performed using the Instron 3369 Universal Testing Machine (crosshead speed of 1 mm min^{-1}). For this, cement pastes were poured into a cylindrical silicone mold with the dimensions 8 mm x 16 mm, then maturated (2 days) and dried (5 days) in a humid atmosphere at 37°C. All values in this investigation are the means of three samples.

2.4. Antibiotic release kinetics

Antibiotic release tests on the cements were performed in accordance with the European Pharmacopoeia standards. For this purpose, the tests were carried out using a Dissolutest apparatus (Pharmatest®) equipped with a rotating paddle stirring system adapted to parallel bowls and controlled temperature.

The ciprofloxacin release tests were performed on dried (D) and fresh (F) cylindrical cements (10mm / 10mm) in order to examine the effect of microstructure and composition on the elution of the active ingredient. The fresh cements were introduced into the release medium 2h after their preparation (slightly longer than the cement's final setting time). While the dried cements were introduced after maturation for 48 hours at 37°C in a humid medium before being dried for five days in an oven at 37°C.

The composite cement (RCC-D) without Ciprofloxacin was also introduced in the release medium to verify the existence of any interference between the components of this cement (Phosphate, calcium and carbonates ions, and sodium alginate) and ciprofloxacin molecules.

Each cement sample was immersed in a container containing 1 L of PBS solution adjusted to physiological pH (pH = 7.4). The containers were lidded, and the solution was then stirred for 18 days at a speed of 50 rpm, allowing for homogenization of its composition in all bowls and throughout the trial. Every day, 5 mL of solution was sampled. The antibiotic amounts released were determined by UV spectrophotometry at 270 nm. The solution collected from the release medium of RCC-D was also analyzed.

The composition of the antibiotic-loaded cements tested in this study is presented in Table 2.

Journal Pre-proofs

Table 2. Composition of the different cements prepared and tested in the release study.

Cements	Powder phase				Liquid phase	L/P
	$CaCO_3$ (wt %)	DCPD (wt %)	BG (wt %)	Cip (*wt %)		
RCC-D	37.5	37.5	25	0	5 wt % Alg in Na_2HPO_4 (0.25M)	0.7
RCC-Cip3-D	36	36	25	3		
RCC-Cip9-D	33	33	25	9		
RCC-Cip3-F	36	36	25	3		
RCC-Cip9-F	33	33	25	9		

***:** *wt % of Cip was calculated with respect to the solid phase.*

2.5. Post-release characterization of composite cements

In order to evaluate the evolution of the microstructure and composition of the cements after 18 days of soaking in the PBS solution. The characterization of the dried and fresh cements (RCC-Cip3-D, RCC-Cip3-F) after release was performed using XRD, FTIR, and SEM. It should be noted that the cements after the release test were dried for 5 days at 37°C in the oven. To evaluate the stability of the ciprofloxacin molecule, HPLC-MS analysis (A SHIMADZU LC-MS 8050, Shimadzu, Japan) was performed for pure ciprofloxacin and the solution collected from the release medium (after 18 days). Two solutions were analyzed: the standard ciprofloxacin solution with a concentration of 15/mg/L and ciprofloxacin solution (23mg/L) collected after 18 days of the release test.

2.6. Antibacterial activity

The antibacterial activity of the prepared dry cements (RCC, RCC-Cip3-D, and RCC-Cip9-D) was evaluated in vitro by disk diffusion test using bacterial strains, namely, Staphylococcus as a Gram-positive bacterial strain and Escherichia coli as a Gram-negative bacterial strain. Firstly, cylindrical composite cements (6 mm diameter × 5 mm height) were immersed for 24 hours in 5 ml of sterilized ultrapure water. Then, 50 µl of the supernatant was added into the sterilized absorbent filter paper disk (5 mm diameter × 1 mm height) and impregnated with it for some time. The bacteria were incubated in tryptone soy broth (TSB) medium for 12 hours with agitation before being diluted in 100ml of TSB. The bacteria were then placed in sterile Petri dishes at room temperature and allowed to solidify. The supernatant-containing paper disk filters were placed on the surface of the Petri dishes inoculated with the selected bacteria. After 24 h of incubation at 37 °C, photographs were taken with a digital camera. The effect of the

ciprofloxacin dose was evaluated by measuring the bacterial inhibition zone diameter of the samples (3 samples for each composition). Ciprofloxacin-free samples were used as references. The zone of inhibition diameter was calculated according to the following formula (Eq 2):

$$Inhibition\ zone\ diameter\ (mm) = \frac{(Øiz - Ød)}{2} \qquad \text{(Eq 2)}$$

Where Øiz (mm) is the inhibition zone diameter and Ød (mm) is the filter paper disc diameter.

3. Results & Discussions

3.1. Physicochemical characterization of ciprofloxacin-loaded cement

- **X-Ray Diffraction and Infrared Spectroscopy analyses**

Figure 1 depicts the XRD patterns of the composite cements RCC-Cip3 and RCC-Cip9 compared to those of the composite cement CPC-BG-Alg-NaP, vaterite, bioactive glass (BG), and ciprofloxacin. The X-ray diffractogram of ciprofloxacin revealed that it exhibited a crystalline structure with main peaks (the most intense) at 14.4°, 16.4°, 20.7°, and 25.2° corresponding respectively, to the indices (101), (111), (020), and (121). The reference cement RCC was elaborated from the mixture of reactive powders: brushite, vaterite, and bioactive glass. The XRD diagram of the reference cement (RCC) attested that the dissolution of these reagents within a paste resulted in the precipitation of a nanocrystalline apatite phase as well as the presence of residual vaterite. The diffractograms of the ciprofloxacin-loaded composite cements appeared to be similar compared to the reference cement revealing the presence of apatite as well as residual vaterite. Moreover, there were no peaks of ciprofloxacin on the diagrams, which could be due to the low incorporated amount in the cements. However, it should be noted that the intensity of the apatite peaks formed situated at 26° and 32.2° (2 Theta degree) decreased with the incorporation of ciprofloxacin, and this effect is dose-dependent indicating that the addition of this antibiotic affected the apatite formation. This effect will be thoroughly discussed in the section on the setting reaction kinetics.

Journal Pre-proofs

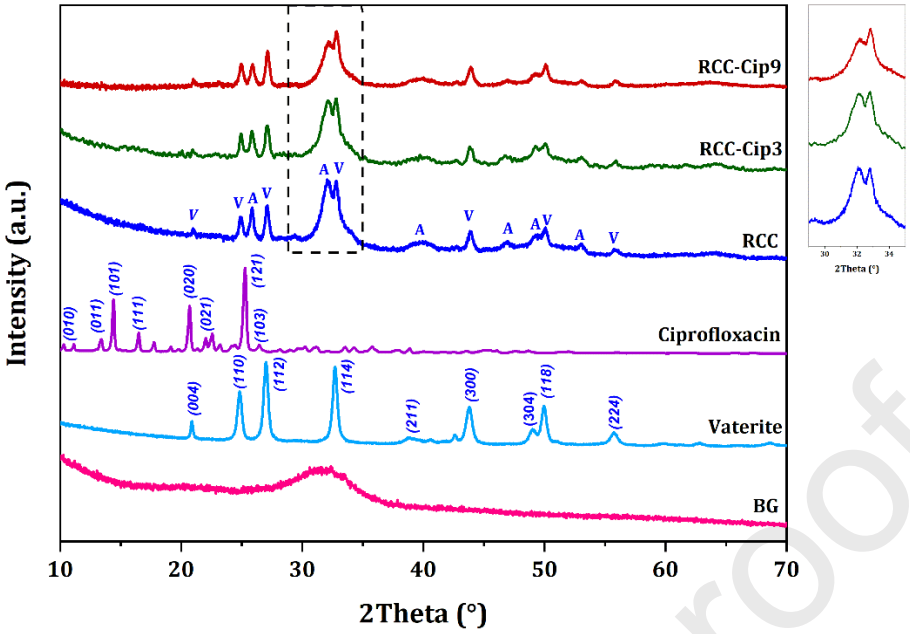

Figure 1. X-ray diffractograms of RCC-Cip3 and RCC-Cip9 composite cements compared with RCC, vaterite, bioactive glass, and ciprofloxacin.

Figure 2. illustrates the FTIR spectra of RCC-Cip3 and RCC-Cip9 composite cements compared to those of RCC composite cement, and ciprofloxacin.

FTIR spectrum of ciprofloxacin which indicated the presence of two bands with an average intensity around 3380 and 3527 cm^{-1} attributed to the OH group of the acid. The bands corresponding to the C-H vibration modes appeared in the range 3015 - 3392 cm^{-1}. Two intense elongation bands were noted around 1712 and 1675 cm^{-1} attributed to the vibrations of the acid function and the carbonyl group, respectively. The spectrum also revealed bands typical of the νCOOH and δC-OH vibrations of the carboxyl group and C-N in the region 1268 and 1317 cm^{-1}. A band with a medium intensity located at 1029 cm^{-1} attested to the presence of the C-F bond. Vibrational bands characteristic of aromatic C=C and N-H bonds were observed around 805 and 750 cm^{-1}, respectively.

The FTIR spectra of the composite cements RCC-Cip3 and RCC-Cip9 when compared to the composite cement RCC, attested the presence of the typical bands of the newly formed apatite phase in the region of 511 - 658 cm^{-1} and 926 - 1240 cm^{-1} which were attributed to the ν4 PO_4 and ν3 PO_4 vibrations of the phosphate group, respectively. Moreover, the characteristic bands of residual vaterite were also visible on the FTIR spectra, at 876 cm^{-1}, and in the range, of 1334-1590 cm^{-1} attributed respectively to the ν2 CO_3, and ν3 CO_3 vibration of the carbonate group. It should be noted that the incorporation of ciprofloxacin appeared to affect the intensity and width of the ν_2 CO_3 band (at 876 cm^{-1}), which became more intense and less broad. In addition

to the phosphate and carbonate bands, the FTIR spectra of RCC-Cip3 and RCC-Cip9 cements revealed the presence of the new characteristic bands of ciprofloxacin in the region 805 cm^{-1}, 1268 cm^{-1}, 1317 cm^{-1} attributed to the C=C, vCOOH, and δC-OH, and C-N vibrations, respectively. The FTIR spectrum of the RCC-Cip9 composite cement was marked by the presence of the C=O vibrational band around 1675 cm^{-1} which is characteristic of ciprofloxacin.

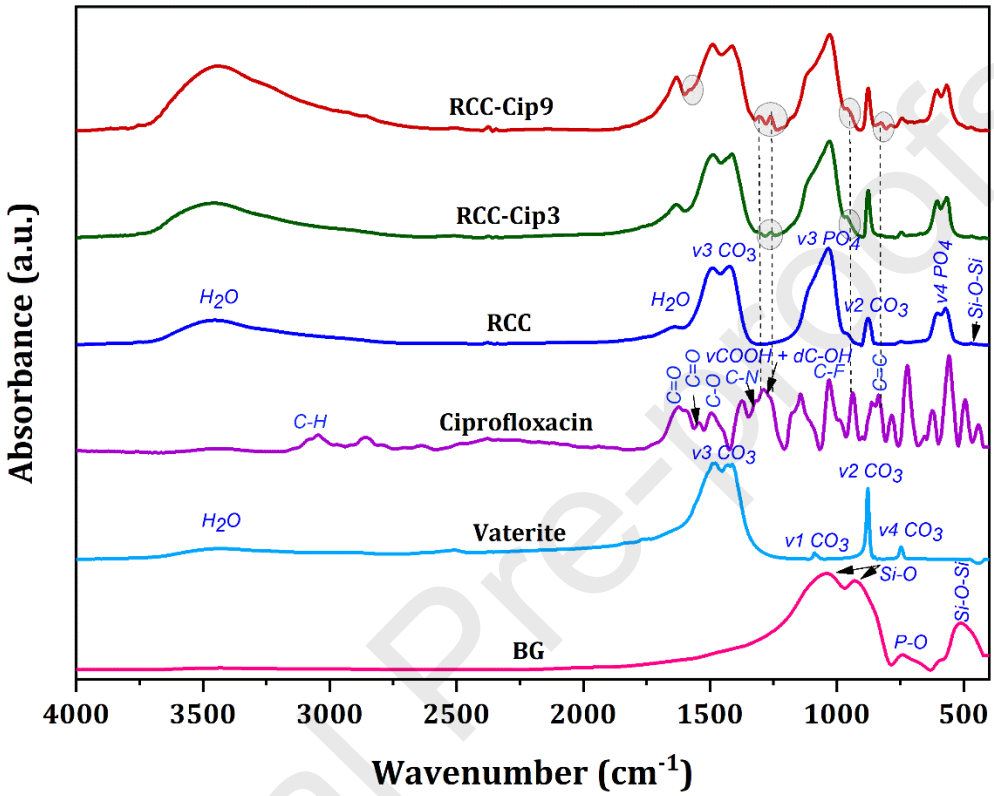

Figure 2. FTIR spectra of RCC-Cip3, RCC-Cip9 composite cements compared to RCC, vaterite, bioactive glass, and ciprofloxacin.

- **Morphology examination and mercury intrusion porosity measurements**

The morphology of the hardened cements was analyzed by scanning electron microscopy and presented in Figure 3. SEM analysis revealed that the BG glass powders had a morphology of blocky particles. Figure 3.B of the vaterite showed particles in the shape of "lenses", ranging in size from 0.5 to 2 µm.

The SEM image of pure ciprofloxacin powder revealed that this active ingredient was visible as irregular crystalline aggregates in the form of rod-like crystals (Figure 3.C). The EDX spectrum showed the presence of peaks of the elements C, O, N, and F, which were typical of ciprofloxacin (Figure 3.D).

The analysis was performed at the 100 µm scale in order to evaluate the surface of the prepared cements and, in particular, to assess the porosity. The results of the surface examination showed

Journal Pre-proofs

that the cement formulated without ciprofloxacin (RCC) had the densest structure (Figure 3.C) and the ciprofloxacin-loaded composite cements exhibited a porous structure (Figure 3.I and 3.M). Furthermore, the images at higher magnifications (x10.000) attested to the modification of the surface of the cement with the incorporation of Cip revealing the appearance of microporosity (Figure 3.J, 3.K, 3.N, and 3.O) and crystals in the form of rods typical of ciprofloxacin (green arrows) for the composite RCC-Cip9 (Figure 3.O) as well as the presence of block-like particles typical to the bioactive glass (pink arrows) and needle-like crystals attributed to the precipitated apatite (orange arrows). The EDX spectra of RCC-Cip3 and RCC-Cip9 revealed the appearance of the fluoride element pic, which was indicative of the presence of ciprofloxacin in the cement composites.

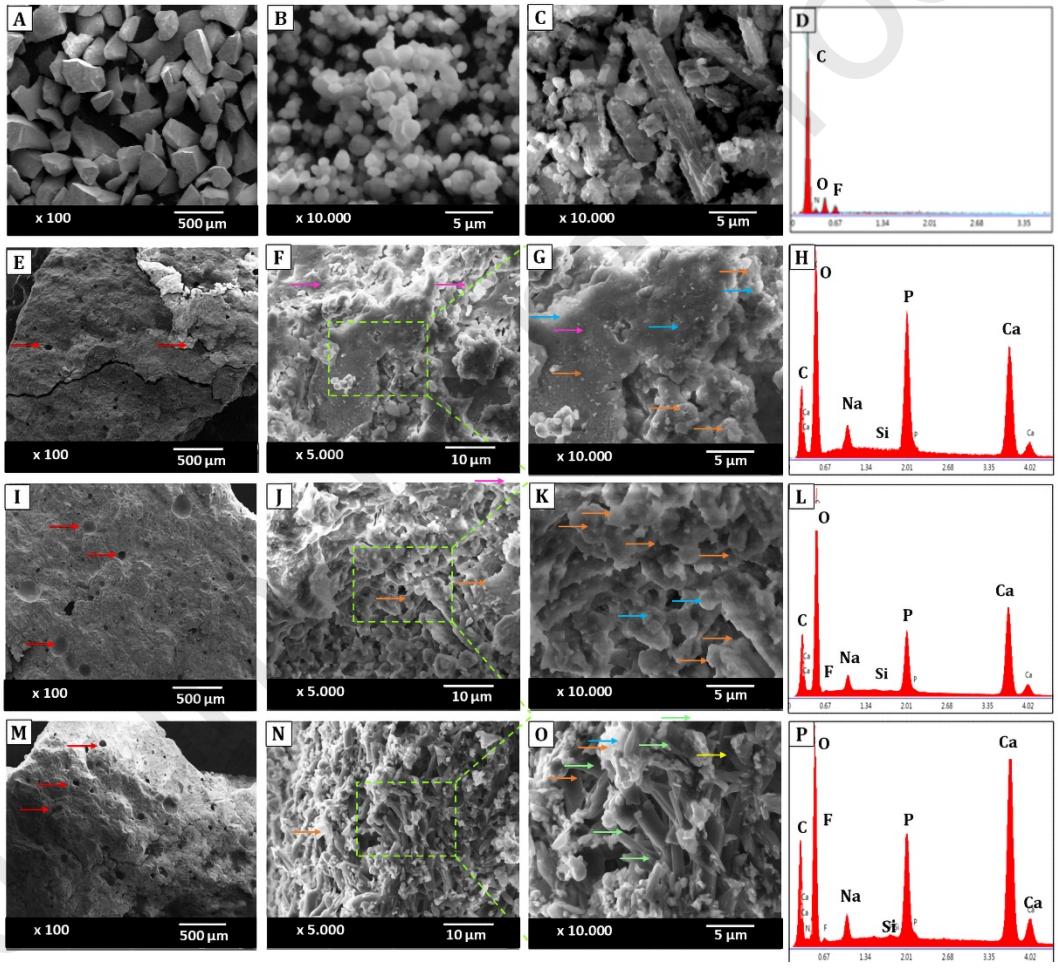

Figure 3. SEM images and EDX spectra of bioactive glass BG (A), vaterite (B), ciprofloxacin (C and D), RCC (E, F, G, and H), RCC-Cip3 (I, J, K, and L), RCC-Cip9 (M, N, O, and P) composite cements. Red arrows (Pores), pink arrows (BG), orange arrows (Apatite), blue arrows (vaterite), and green arrows (ciprofloxacin).

Characterizing the porosity of CPCs is a critical step in efficiently correlating their structural features with their relevant properties, including in vitro or in vivo activity, drug release kinetics, or degradation behavior.

The porosity measurements of the prepared cements are illustrated in table 3. The results revealed that the incorporation of ciprofloxacin antibiotic into the composite cement matrix increased the total pore area from a value of 38.4 m^2/g for the RCC cement to a value of 68.5 m^2/g and 84.7 m^2/g for RCC-Cip3 and RCC-Cip9, respectively. Furthermore, the porosity rate did not appear to have a significant effect by the incorporation of ciprofloxacin molecules, which slightly increased from a value of 53.2% for the RCC and the same value was recorded for the RCC-Cip3 cement and increased to a value of 55.2% RCC-Cip9.

Figure 4 depicts the pore size distribution of the prepared cements. The results of the pore size distribution of RCC cement, revealed the presence of four populations. The first range at larger pore sizes is located between 10 - 50 μm which could be due to the voids formed between the different constituents of the cements after the setting reaction. The second one ranges from 100 nm to 1 μm, and the range of 40 – 100 nm, and the smaller pore size range inferior to 40 nm.

At first glance, some changes in the porosity curves were noted, including the width, height, and position of the pore distributions with the addition of ciprofloxacin into the reference cement (RCC) attesting to the decrease of the pore size diameter and this effect was dose dependent. Indeed, the incorporation of ciprofloxacin (3 and 9 wt%) resulted in the disappearance of a larger pore size range (10 - 50 μm) and decreased the pore size range between 0.1 and 1 μm and the related peak was shifted towards smaller pore size values and a decrease in its intensity, by the increase of ciprofloxacin content. This effect could be related to the presence of ciprofloxacin particles that occupied and filled the pores. However, the incorporation of ciprofloxacin appeared to increase the pore sizes which were inferior to 100 nm (the range between 40 – 100 nm and the pore size population inferior to 40 nm) attesting that the incorporation of ciprofloxacin favorized the formation of nanoporosity, and this effect was dose-dependent. This effect was also noticed by the increase of the total pore area from a value of 38.4 m^2/g for RCC cement to 68.5 and 84.7 m^2/g for RCC-Cip3 and RCC-Cip9, respectively.

On the other hand, the large pores observed in the SEM micrographs (Fig. 3) were not identified in the Mercury Intrusion Porosity measurements (Fig. 4), which recorded only submicrometer pores, this could be regarded as a technique limitation (Pastorino et al., 2015b). This range of pore sizes is critical in drug delivery applications, for biomolecules loading and release.

Table 3. Porosity parameters of prepared composite cements.

Parameters	RCC	RCC-Cip3	RCC-Cip9
Total pore area (m^2/g)	38.4	68.5	84.7
Porosity (%)	53.2	53.2	55.8

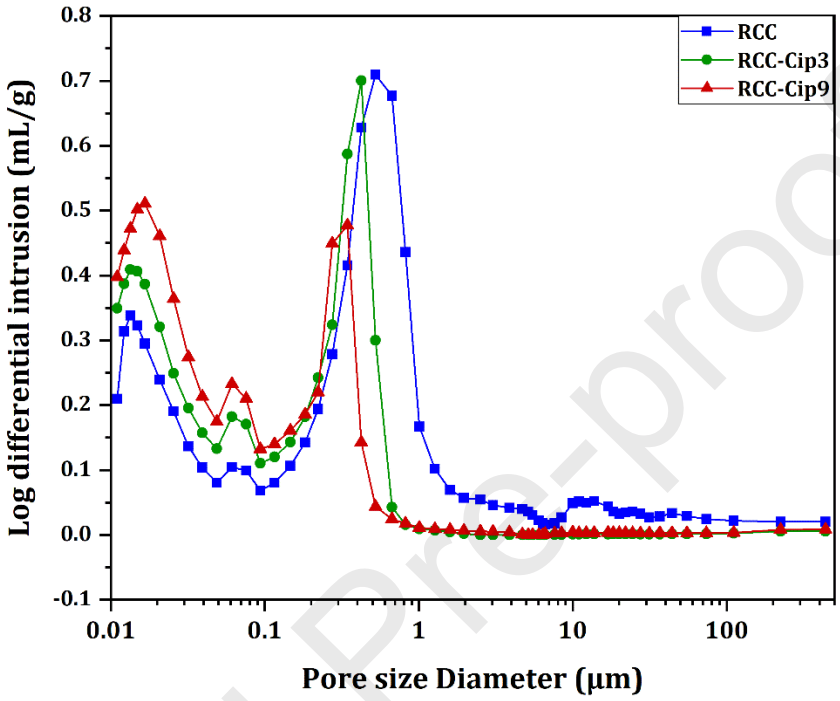

Figure 4. Pore size distribution of reference cement (RCC) and cements filled with 3% and 9% Cip (RCC-Cip3 and (RCC-Cip9).

3.2. Evaluation of the properties of the ciprofloxacin-loaded cement

3.2.1. Effect of ciprofloxacin and its content on the setting properties of composite cement

- **Kinetics of the setting reaction**

The effect of ciprofloxacin incorporation on the setting reaction of RCC composite cement was evaluated using X-ray diffraction (10 - 55°) after different reaction times in order to follow the evolution of apatite formation in composites formulated in the presence of two doses of ciprofloxacin 3 and 9 wt%. The setting kinetics were assessed by following the evolution of the XRD peaks of brushite as the limiting reagent and apatite as a product of the setting reaction. The evolution of the X-ray diffractograms of RCC-Cip3, and RCC-Cip9 compared to RCC reference cement, as a function of the reaction time (2, 4, 6, 24, and 48h), is shown in Figure 5.

Journal Pre-proofs

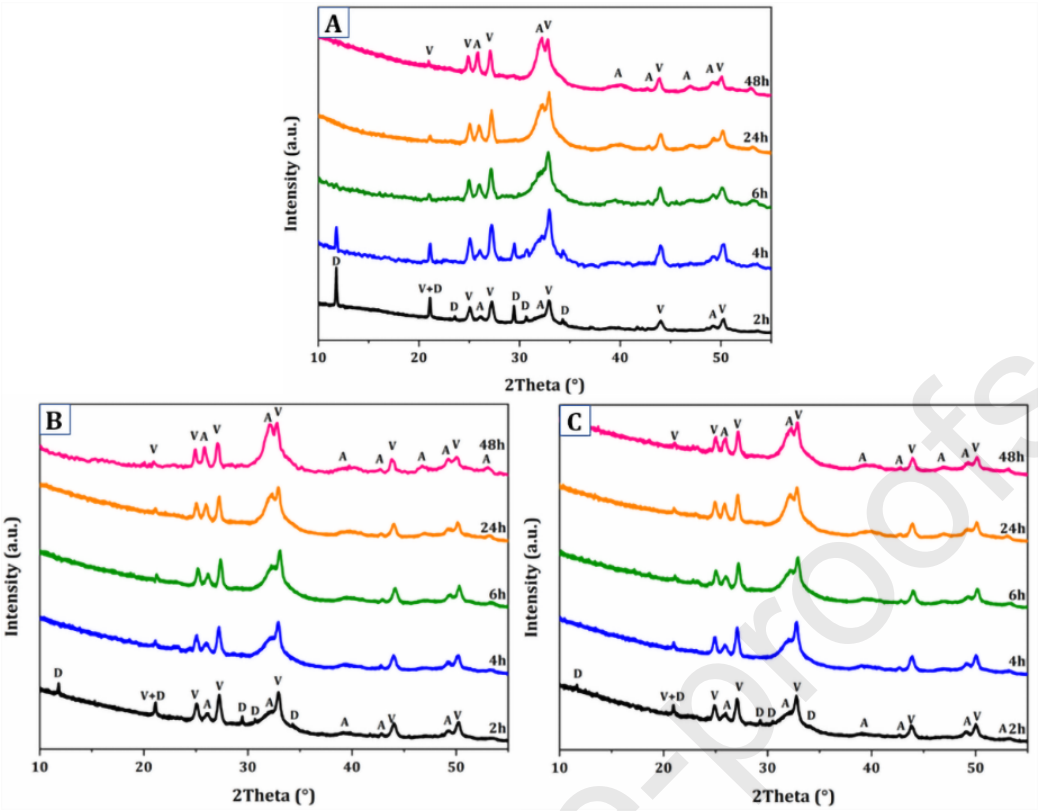

Figure 5. evolution of X-ray diffractograms during the setting of the cements RCC (A), RCC-Cip3 (B), RCC-Cip9 (C).

The evolution of the diffractograms of the composite cement RCC (figure 5.A) showed the presence of characteristic peaks of brushite, vaterite, and apatite phases after 2 and 4 hours of reaction. After 6 hours, the peaks attributed to the presence of residual vaterite, and apatite formed were all indexed on the diffractogram with the total disappearance of the peaks corresponding to the brushite. The evolution of the diffractograms of the ciprofloxacin-loaded cements, RCC-Cip3 and RCC-Cip9 (figure 5.B and 5.C) revealed rapid kinetics during the first hours compared to that of the RCC cement. Indeed, after only 4 hours of reaction, the typical brushite peaks have all disappeared and only the characteristic peaks of residual vaterite and precipitated apatite were recorded on the diffractograms. It should be noted that during the first hours (2, 4, and 6h) the apatite peaks, particularly those located at 26° and 32.2°, showed a higher intensity for the ciprofloxacin loaded-cements (RCC-Cip3 and RCC-Cip9) compared to the RCC cement. However, after 48 hours of reaction, the diffractograms revealed a higher intensity of apatite peaks for the composite cement RCC compared to the cements RCC-Cip3 and RCC-Cip9.

In order to monitor the evolution of the apatite phase during the setting reaction of the cements formulated in the presence of ciprofloxacin, a peak area ratio of the apatite (26°) and vaterite

(25.2°) peaks was calculated using the Origin software. Figure 6 depicts the apatite/vaterite area ratio (A_{Ap}/A_{Vat}) as a function of reaction times for RCC-Cip3, and RCC-Cip9 cements compared to RCC composite cement. The results showed that after 2 hours the ratio was maximum with a value of 0.836 for the RCC-Cip9 cement, followed by the RCC-Cip3 composite with a ratio value of 0.782 while the RCC composite had the lowest ratio (0.693). After 4 hours of reaction, the ratio increased for all the composite cements; and RCC-Cip3, RCC-Cip9 composites had nearly the same area ratio which is 0.933 and 0.934, respectively. The area ratio of the composite cement RCC was 0.737. The same trend was noted after 6 hours of reaction, the two loaded cements had almost the same ratio (0.968 and 0.969 for RCC-Cip3 and RCC-Cip9 cements, respectively). The area ratio of the three composite cements RCC, RCC-Cip3, and RCC-Cip9 appeared to be the same after 24 hours of reaction with a slight increase for the ciprofloxacin-loaded cements; the ratio values are, 0.999, 0.995, and 0.992, respectively. After 48 hours of reaction, the ratio increased significantly for RCC cement and reached a maximum value of 1.234, while it increased slightly for the loaded cements which had ratios of 1.006 for RCC-Cip3 cement and 0.996 for RCC-Cip9 cement which had the lowest area ratio.

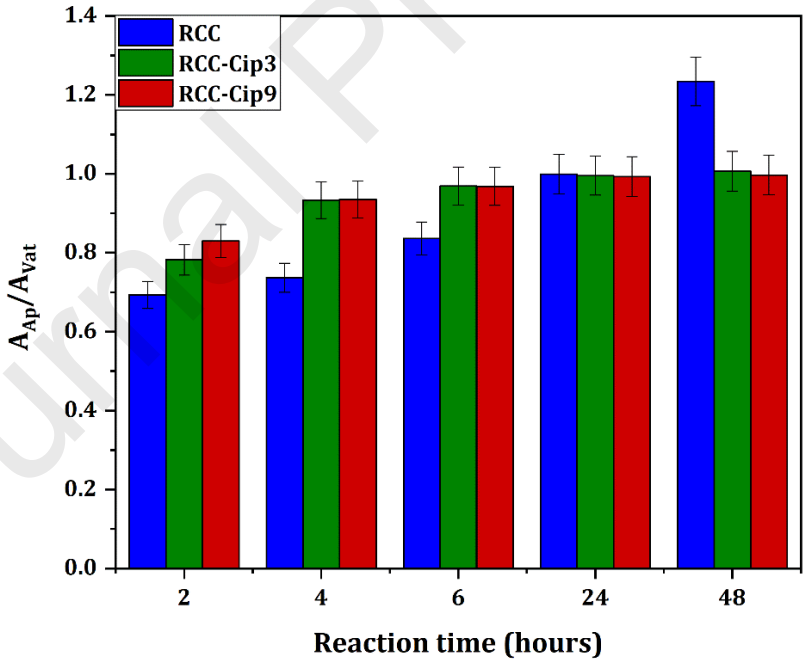

Figure 6. Area ratio A_{Ap}/A_{Vat} during setting of RCC, RCC-Cip3, and RCC-Cip9 cements.

The results of the XRD analysis revealed that the incorporation of ciprofloxacin seemed to influence the kinetics of the cement setting reaction, thus favoring the precipitation of apatite

Journal Pre-proofs

during the first hours of the reaction and after 48 hours, the apatite formation was affected by increasing the amount of ciprofloxacin.

Indeed, the setting reaction of RCC cement was based on the existence of several chemical mechanisms that led to the formation of apatite, namely the reaction between vaterite and brushite and the reaction between bioactive glass and brushite, as well as the reaction between the calcium and phosphate ions of BG and the ions resulted from the dissolution of brushite and vaterite.

The acceleration of apatite formation during the first hours of the reaction that occurred with the addition of ciprofloxacin could be due to the presence of fluoride in the ciprofloxacin molecule resulting in a fast apatite formation. It was found that the presence of small amounts of fluorides in the mixing solution of calcium phosphate cements based on β-TCP-DCPD-$CaCO_3$ resulted in an increased rate of DCPD and $CaCO_3$ conversion and consequently apatite formation. This effect was explained by an initial precipitation of fluorapatite crystals formed which can act as seeds for the subsequent growth of apatite, increasing the rate of reaction (Mirtchi et al, 1991). It was reported also that fluoride-doped calcium silicate cement (composed of Ca_2SiO and Ca_3SiO_5, $Ca_3Al_2O_6$, $CaSO_4$, $CaCl_2$, and Bi_2O_3) has revealed accelerated apatite formation with the earlier formation of fluorapatite (Ranjkesh et al., 2016). Shah et al., reported that the presence of F^- ions in low concentrations were found to accelerate apatite formation on the surface of 45S5 bioglass (Shah et al., 2015).

The decrease of the amount of apatite formed after 48 hours, as confirmed by the calculated area ratio (which decreased from a value of 1.234 for the reference cement to 1.006 and 0.996 by increasing the amount of ciprofloxacin for 3 and 9 wt%, respectively) could be due to the presence of a competing reaction between ciprofloxacin and the calcium ions existing in the matrix. Indeed, the presence of the carboxyl R-COOH group of the ciprofloxacin molecule in its anionic form (figure 7) due to the basic pH (pH>9) of the liquid phase can interact with the positively charged calcium ions (Ca^{2+}) resulting in "chelation" and leading to the consumption of a part of calcium ions.

Several authors have claimed the effect of some organic molecules on the formation of apatite and brushite cements. Mabroum et al., discussed the effect of alginate on the formation of apatite phase and suggested that the delaying effect of this polymer on the precipitation and formation of apatite could be due to the formation of calcium alginate because of the presence of the COO- group resulting in the ionic exchange of Na and Ca (Mabroum et al., 2022, 2021). Alkhraisat et al., reported that low concentrations of tetracyclines can produce calcium chelates that affected primary nucleation, which interfered with mineral precipitation, resulting in a

delay effect in the setting reaction for both apatite (Ratier et al., 2004, 2001) and brushite cements (Alkhraisat et al., 2010).

Canal et al., reported that the incorporation of doxycycline hyclate in the CPC based on α-TCP modified the physicochemical properties attesting that it slightly delayed the reaction due to the initial deceleration of the setting reaction produced by the incorporation of Doxy which did not prevent the hydrolysis of α-TCP to apatite phase, as only some traces of α-TCP were found in the Doxy-containing cements (Canal et al., 2013b).

This effect was also observed in a study conducted by Takechi et al., who investigated the effect of incorporating flomoxef sodium on apatite formation in TTCP and DCPA-based-cement. They noted an inhibitory effect on apatite formation that increased with increasing flomoxef sodium doses (Takechi et al., 2002).

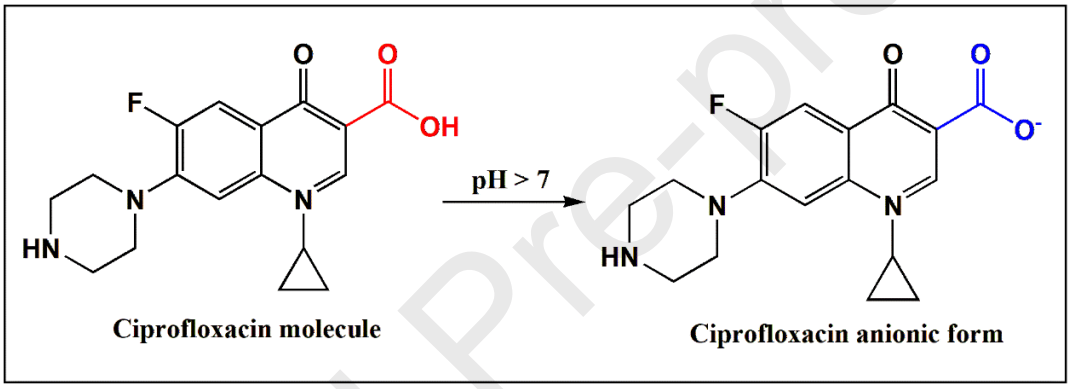

Figure 7. Structure of ciprofloxacin molecule and ciprofloxacin anionic form.

- **Setting time**

Table 4 illustrates the initial and final setting times of the composite cements RCC, RCC-Cip3, and RCC-Cip9. The results showed that the incorporation of ciprofloxacin slightly prolonged the setting time, and this effect was dose-dependent. Indeed, the initial (ti) and final (tf) setting times of the RCC composite cement increased from 10 minutes (ti) and 22 minutes (tf) to an initial setting time of 14 minutes and a final setting time of 25 minutes for the RCC-Cip3 cement. RCC-Cip9 cement had the longest setting times with initial and final setting times of 17 minutes and 29 minutes, respectively. Generally, the introduction of an antibiotic, in the liquid or solid phase during the formulation of various calcium phosphate cements, is accompanied by an increase in setting time. Hesaraki et al., investigated the effect of the incorporation of cephalexin on the physicochemical properties of a TTCP and DCPD-based cement. The results showed that the setting time was extended with the incorporation of this antibiotic (Hesaraki and Nemati, 2009). Similarly, Canal et al., reported that the incorporation

of doxycycline hyclate into the liquid phase of an α-TCP-based CPC and attested to an extension of the setting time from 11 to 71 minutes (Canal et al., 2013a). Kisanuki et al., found that the incorporation of dideoxy-kanamycin B into Biopex-R6.7 cement (a mixture of α-TCP, TTCP, HA, and Mg_2PO_4) was prolonged by adding and increasing the rate of this active ingredient (Kisanuki et al., 2007).

The same findings were reported by Ratier et al., when they investigated the effect of incorporating 7% of tetracycline in a CPC based on α-TCP and glycerophosphate and noted an increase in setting time from a value of 19 minutes to 43 minutes (Ratier et al., 2001). The increase in setting time observed by these authors was attributed to the interaction of the antibiotic with the solid phase of the cement during setting, which delayed the process of conversion of the reagents into the apatite phase.

The results obtained in our study indicated that even if the antibiotic prolonged the setting time, it remained in the 10–40 min range that is required by the clinicians.

Table 4. Initial and final setting times of RCC, RCC-Cip3, and RCC-Cip9 composite cements.

Cements	Initial setting time (min)	Final setting time (min)
RCC	10 ± 2	22 ± 2
RCC-Cip3	14 ± 2	25 ± 3
RCC-Cip9	17 ± 3	29 ± 3

3.2.2. Effect of ciprofloxacin on the cohesion and injectability of composite cement pastes

- **Cohesion**

The cohesion of the pastes of the antibiotic-loaded cements was assessed visually by monitoring the state of the cement pastes in PBS solution (disintegration or not of the paste). The results of the cohesion test of RCC-Cip3 and RCC-Cip9 cements compared to RCC composite cement are shown in Figure 8. Photos taken after 5 minutes and 24 hours of immersion in PBS solution revealed that the RCC composite cement has not disintegrated, and the paste has retained its shape and hardened in PBS solution even after 24 hours of immersion. The incorporation of ciprofloxacin appeared to have no effect on cement cohesion, as the pastes of RCC-Cip3 and RCC-Cip9 cements demonstrated excellent cohesion with no turbidity or disintegration, and the cement pastes of the ciprofloxacin-loaded cements completely hardened in the PBS solution.

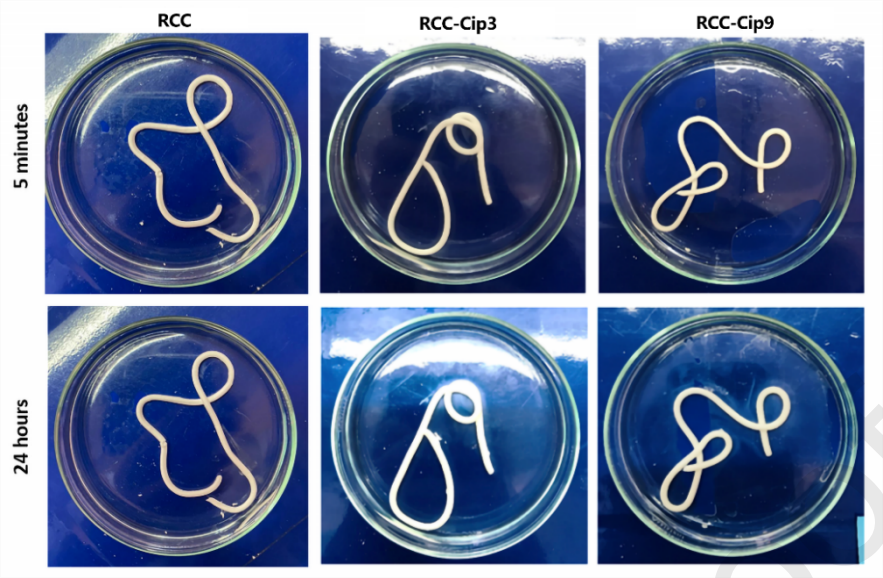

Figure 8. Photos of the pastes of RCC, RCC-Cip3, and RCC-Cip9 composite cements injected into the PBS solution. Photos were taken after 5 min and 24 h of immersion.

- **Injectability**

Figure 9 depicts the results of the assessment of the injectability of ciprofloxacin-loaded cements. The obtained results showed that the composite cement RCC had an injectability of approximately 98%, attesting to its good injectability. The addition of Cip did not appear to have a significant effect on injectability. The results of the injectability measurement of RCC-Cip3 and RCC-Cip9 cements, when compared to RCC composite cement, showed a slight decrease with the incorporation of ciprofloxacin (Figure 9). Injectability decreased from a value of 98% for the RCC cement to a value of 97% when incorporating a dose of 3% ciprofloxacin (RCC-Cip3), and 95% injectability for the composite formulated with 9% ciprofloxacin (RCC-Cip9). The high injectability noted for the examined composite cements was attributed to their good cohesion provided by the presence of alginate.

In general, the incorporation of antibiotics into CPCs improves their injectability. The slight decrease in injectability caused by the addition of ciprofloxacin antibiotic could be attributed to a decrease in the viscosity of the cement pastes.

Ratier et al., reported the effect of tetracycline (TTC) on the injectability of a CPC based on α-TCP and glycerophosphate. The measurement of injectability showed that the incorporation of a 7% dose of tetracycline increased injectability nearly twofold, from a value of 31% in the absence of TTC to a value of 62% with the incorporation of 7% of TTC (Ratier et al., 2004).

Noukrati et al., evaluated the effect of sodium fusidate (SF) on the injectability of DCPD-$CaCO_3$-based cement and showed that the injectability of the cement paste containing SF

antibiotic is greater than that of the reference cement; furthermore, the filter-press phenomenon can be prevented by combining an L/P ratio of 0.8 with 9% SF loading (Noukrati et al., 2016). A similar trend was noted for cephalexin-loaded calcium phosphate cement; the authors proposed a lubricating effect of the antibiotic, enhancing the extrusion of the CPC paste (Hesaraki and Nemati, 2009).

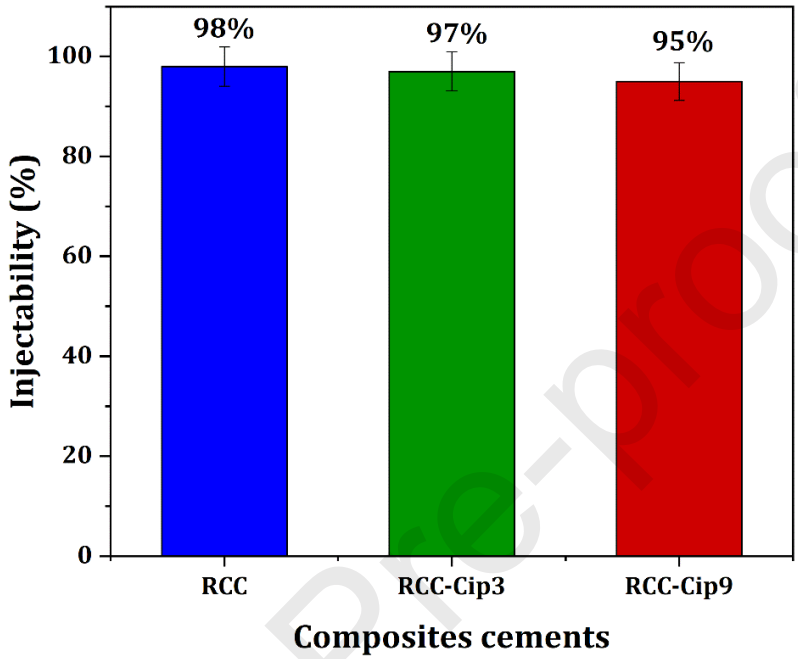

Figure 9. Injectability of RCC, RCC-Cip3, and RCC-Cip9 composite cements.

3.2.3 Effect of ciprofloxacin on the compressive strength of composite cement

Figure 10 shows the compressive strength of RCC-Cip3 and RCC-Cip9 composite cements compared to RCC cement. The results revealed that the incorporation of the antibiotic caused a decrease in compressive strength and this effect was dose dependent. Indeed, the compressive strength of the composite cement RCC was 10.5 ± 1.1 MPa which decreased to a value of 9.1± 1.0 MPa for the composite RCC-Cip3 and 8.1 ± 0.9 MPa for RCC-Cip9. This effect could be attributed to the increase of the total pore area from 38.4 m^2/g and the porosity rate from a value of 53.2% for RCC cement to a value of 84.7 m^2/g and 55.8% for RCC-Cip9, respectively (table 3). This effect could be also related to the appearance of macroporosity as evidenced in the SEM images upon the incorporation of ciprofloxacin which increased with the increase of the antibiotic rate.

Similarly, Noukrati et al, found that the addition of sodium fusidate (9 wt%) in a DCPD-$CaCO_3$-based cement slightly reduced the compressive strength of the cement from 11.8 to 9.3 MPa for L/P = 0.7 and from 4 to 3.4 MPa for L/P = 0.8 (Noukrati et al., 2016). Wu et al., reported that

a CPC-chitosan composite cement containing 50% penicillin-encapsulating alginate microbeads exhibited a decrease in flexural strength compared to the CPC-chitosan control from 7.1 ± 1.3 to 3.16 ± 0.55 MPa (Wu et al., 2021). Daley et al., evaluated the effect of doxycycline on the mechanical strength of a calcium phosphate cement (Hydroset). The results showed a decrease in Young's modulus with increasing doxycycline content from a value of 1350 MPa in the absence of the antibiotic to 1250 MPa for a concentration of 10mg/ml and 1170 MPa for 15mg/ml (Daley et al., 2018).

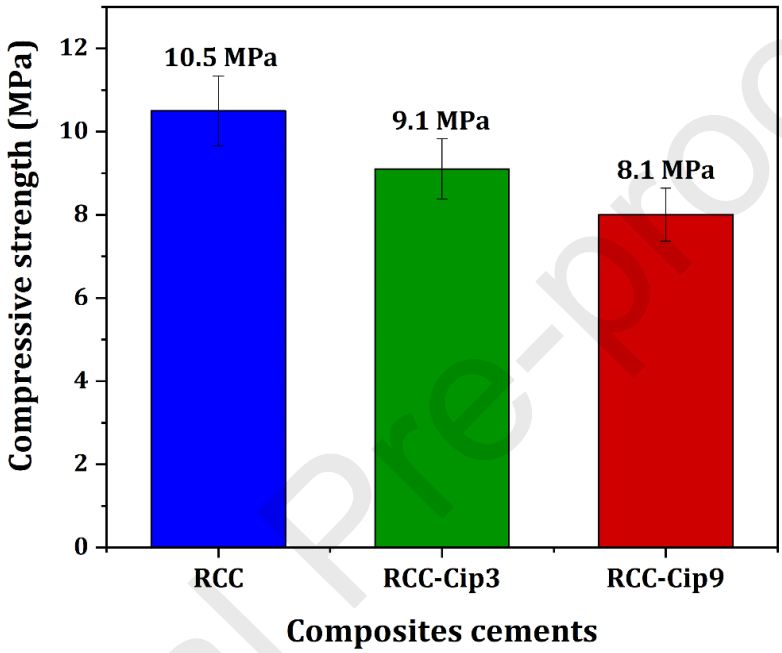

Figure 10. Compressive strength of RCC, RCC-Cip3, and RCC-Cip9 composite cements.

3.3. Antibiotic release study

The main objective of the release study was to investigate the effect of ciprofloxacin dose and cement state on the release kinetics of ciprofloxacin. As a first step, the determination method of ciprofloxacin was validated. For this, absorption spectra of the solutions collected after 18 days for the composite cement (RCC-D) and ciprofloxacin-loaded cement (RCC-Cip3-D) were performed to study the effect of any potential interference between the species resulting from the dissolution of the cement composites (phosphate ions, carbonates, calcium, alginate, and bioglass) and the ciprofloxacin molecules.

Figure 11 shows the obtained absorption spectra of the solutions of the composite cement (RCC-D) and ciprofloxacin-loaded cement (RCC-Cip3-D) after 18 days of release test compared to a ciprofloxacin solution as a standard (23 mg/L of Cip prepared in PBS solution with a pH of 7.4). The absorption spectrum of the standard solution showed the presence of the

maximum absorbance at a wavelength of 270 nm. The absorption spectrum of the solution collected for the RCC-Cip3-D composite cement seemed to be similar to that of the standard solution attesting to the presence of the maximum absorbance at the same wavelength (270 nm). Furthermore, the solution taken from the medium containing the composite cement without ciprofloxacin (RCC-D) showed no absorbance in the examined range, attesting to the absence of interference between the cement constituents and the ciprofloxacin molecule.

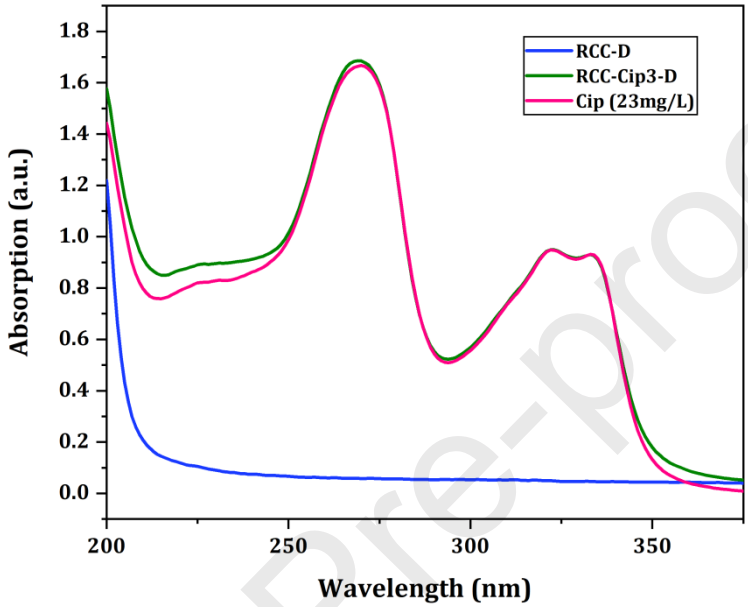

Figure 11. Absorption spectra of the solutions collected after 18 days for the composite cement (RCC-D) and cement (RCC-Cip3-D) loaded with the antibiotic (23 mg/L) compared to the ciprofloxacin solution standard (23 mg/L).

3.3.1. Effect of ciprofloxacin dose on release kinetics

The effect of ciprofloxacin dose (3% and 9%) on release kinetics was first investigated in the dried composite cement RCC-D. The evolution of the cumulative amounts released (%) of ciprofloxacin by the dried composite cements (RCC-Cip3-D and RCC-Cip9-D) as a function of time is presented in Figure 12.

The obtained results attested that the antibiotic is progressively eluted during the release period for both composites with an initial burst release of Cip during the first day. The elution behavior depended on the dose of ciprofloxacin incorporated. Indeed, the cements containing 3% and 9% ciprofloxacin had different release profiles in terms of the cumulative release (%) and amounts released per day.

The cumulative percentage of active ingredient released by the RCC-Cip3-D cement reached 91% after 18 days, while this rate was around 74% for the RCC-Cip9-D cement.

Journal Pre-proofs

In terms of quantities released per day (Figure 12.B), two distinct release stages were noticed, the first one noted a burst release profile of ciprofloxacin during the first day for both cements revealing a released amount of 8.4 mg/L and 15.2 mg/L, for RCC-Cip3-D and RCC-Cip9-D, respectively. These initial high-release amounts could be explained by the dissolution of the ciprofloxacin molecules located at or near the surface and also the antibiotic occupying the voids and pores of the formulated composites. The second stage was characterized by slower released amounts and a sustained release for the remainder of the test period, attesting that the amounts released remained relatively constant and stabilized in the range of 0.46 to 3.20 mg.L^{-1}/day beginning on day 3.

The findings are in agreement with a study conducted by Hamanishi et al., in which the release of various amounts of vancomycin (1%, 2%, or 5%) from a TTCP-DCPD cement was monitored for a period of 80 days (Hamanishi et al., 1996). The results showed that the time required for the entire antibiotic to be released is strongly related to the amount of antibiotic initially introduced into the cement. Indeed, cements containing 1%, 2%, and 5% vancomycin achieved 100% release after 20 days, 40 days, and 80 days, respectively. Montazerolghaem et al., investigated the release of various doses of simvastatin (SVA) in solid form (0.25 0.5, and 1 mgSVA). from a CPC (Montazerolghaem and Karlsson Ott, 2014). The results revealed prolonged release and the cumulative percentages of release were inversely proportional to the drug dose.

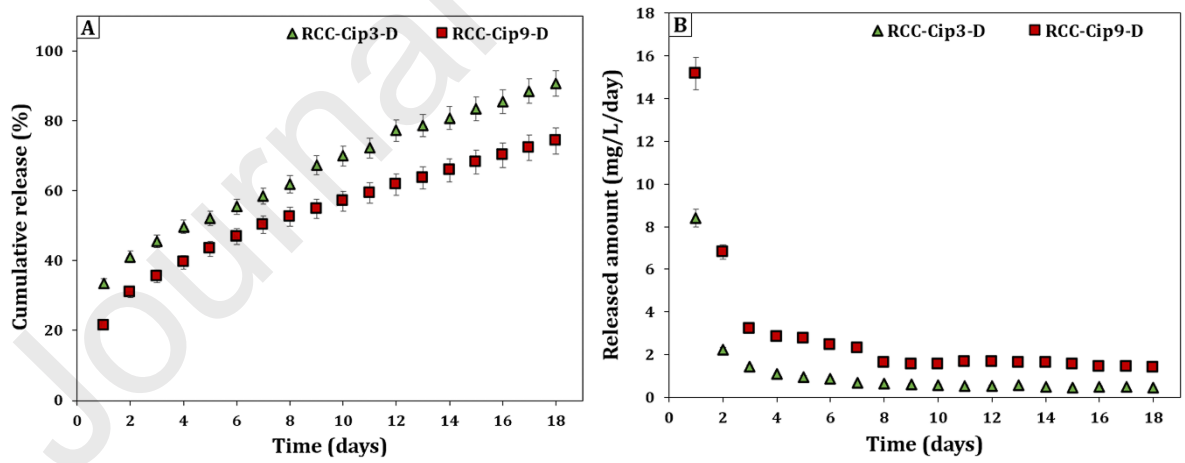

Figure 12. Cumulative release (A) and amount of ciprofloxacin (B) released per day (mg.L^{-1}/day) as a function of immersion time of RCC-D and RCC-Cip9-D.

To identify the mechanisms that governed the release of antibiotics, the obtained data were modeled according to the Korsmeyer -Peppas model (Eq 3).

$$Q = k * t^{n} \qquad \text{(Eq 3)}$$

Journal Pre-proofs

In this equation, **k** is a parameter that defines the matrix's geometrical and structural features, whereas n is associated with the mechanism that governs the release kinetics, the value of this factor indicates the release regime. For cylindrical specimens, the parameter "**n**" of Peppas' model can range between 0.45 and 1, corresponding to a release controlled by multiple simultaneous mechanisms. When **n**=0.45, the release is governed by the diffusion process following Fick's law, and when **n**=1, the release is independent of time, indicating zeroth-order kinetic which is represented by the following mathematical equation (4).

$$\mathbf{Q = K_o * t} \text{ (Eq 4)}$$

Where Q is the fraction of the drug dissolved at a given time t, and K_o represents the constant release rate that remains unchanged throughout the dissolution process.

The values obtained for the exponent "n" (Table 5) were 0.40 and 0.45 respectively, for the composite cement RCC-Cip3-D and RCC-Cip9-D thus revealing that the main mechanism governing the release kinetics of the active ingredient from the two cements was the diffusion mechanism according to Fick's law

Table 5. Comparison of dissolution profiles according to the Korsmeyer - Peppas models.

Model	Equation	Parameters	RCC-Cip3-D	RCC-Cip9-D
Korsmeyer - Peppas	$Q = kt^n$	r^2	0.97	0.99
		n	0.40	0.45

3.3.2. Influence of the cement state on the release kinetics of ciprofloxacin

During surgery, the cements will be implanted as an injectable paste directly after their preparation, hence the interest to study the release of the antibiotic from freshly prepared cements. This section of this research will compare the kinetics of ciprofloxacin release from fresh and dried cements in order to investigate the effect of the microstructure and the composition of the cements on the release of the antibiotic.

The influence of the cement state on the release kinetics was studied for the RCC cement containing the doses of ciprofloxacin, 3 and 9 wt%.

The evolution of the percentages of the antibiotic eluted as a function of time by the cements was investigated (Figure 13). The obtained results demonstrated that the state of the cement significantly influenced the release kinetics. Compared to dried cements, the release profiles of fresh cements appeared to be homogeneous attesting to the absence of the first burst release stage that has been attested for dried cements. The cumulative percentage of ciprofloxacin released rate for the fresh cements decreased from a value of 90.7% for RCC-Cip3-D dried

cement to 76.0 % for RCC-Cip3-F fresh cement, after 18 days of release (Figure 13.A). The same trend was observed for the cements filled with 9% Cip (Figure 13.C) revealing that after 18 days the RCC-Cip9-D cement released a rate of 74.2%, while the RCC-Cip9-F cement released a rate of about 65.4% indicating a gradual release throughout the test period.

When comparing the antibiotic elution kinetics of dried and fresh cements (Figure 13.B and 13.D), the amounts released ($mg.L^{-1}$/day) during the first day were massive for the dried cements loaded with 3 and 9 wt% which were 8.4 mg/L and 15.2 mg/L, for RCC-Cip3-D and RCC-Cip9-D, respectively which decreased critically to 2.2 mg/L and 5 mg/L for RCC-Cip3-F and RCC-Cip9-F fresh cements. Furthermore, fresh cements did not exhibit the phenomenon of burst release on the first day attesting to a gradual and slow release throughout the test duration with amounts released per day varying from 0.2 to 2.2 mg/L and ranging from 1.14 to 2.2 mg/L, for RCC-Cip3-F and RCC-Cip9-F cements, respectively. This difference in release behavior could be related to the pH of the cement pastes. Fresh cements are characterized by the presence of brushite which had an acidic character, lowering the pH of the cement paste and, as a result, the solubility of ciprofloxacin. The low solubility in fresh cements could be the reason for the low release of the antibiotic compared to dried cements with a high pH and thus good solubility of ciprofloxacin.

Moreover, the decrease in the rate of ciprofloxacin released from fresh cements could be attributed to the precipitation of apatite crystals during the setting reaction, filling the voids filled by the liquid containing the drug molecules leading to the inhibition of drug mobility, thus decreasing the release rate (Canal et al., 2013b).

The resulting release profiles were modeled according to the Korsmeyer -Peppas model (Table 6). In comparison to dried cements, where antibiotic release was governed solely by diffusion, the identification of mechanisms involved in the release kinetics from fresh cements appeared to suggest that ciprofloxacin release is not solely controlled by diffusion. The release kinetics pattern of RCC-Cip9-F cement was typical of zeroth-order kinetic which corresponded to a sustained release at a constant rate regardless of ciprofloxacin concentration. In addition, the values of the exponent "**n**" for the two fresh cements were 0.65 and 0.78 (case $0.45<n<1$) for RCC-Cip3-F and RCC-Cip9-F, respectively, indicating that Cip elution occurred in an anomalous manner (non-Fickian) in which, in addition to diffusion, other mechanisms contributed to drug release.

The release mechanisms involved in this case were therefore impossible to determine as the **n** parameter was out of range, which could be due to the modification of the cement matrix over time and setting reaction.

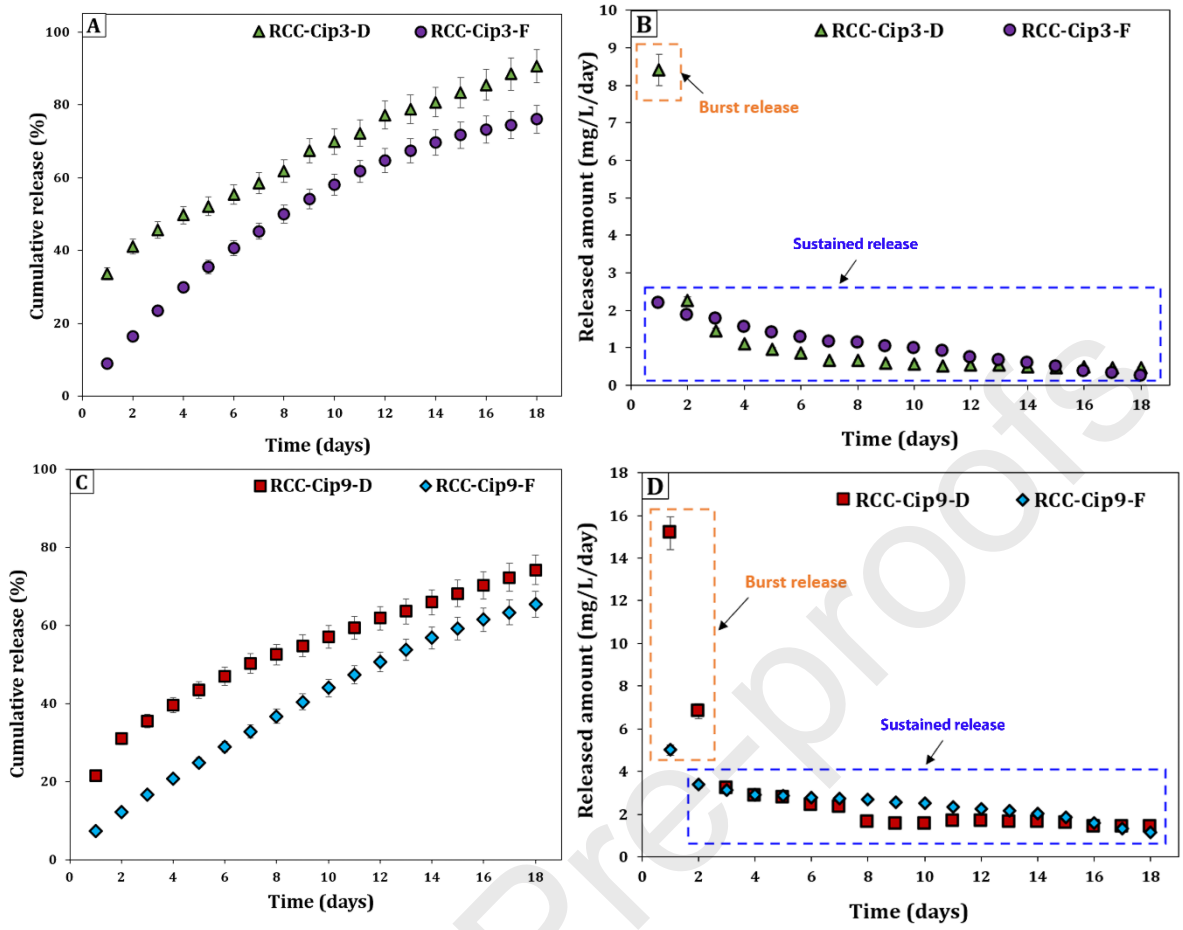

Figure 13. Cumulative release (A) and amount of ciprofloxacin released per day (B) of 3% Cip-loaded cements for RCC-Cip3-D and RCC-Cip3-F and (C) cumulative release and amount of ciprofloxacin released per day (D) of 9% Cip-loaded cements RCC-Cip3-D and RCC-Cip3-F.

Table 6. Comparison of dissolution profiles according to the Korsmeyer - Peppas models.

Model	Equation	Parameter	RCC-Cip3-D	RCC-Cip3-F	RCC-Cip9-D	RCC-Cip9-F
Korsmeyer - Peppas	$Q = kt^n$	r^2	0.976	0.988	0.994	0.998
		N	0.40	0.65	0.45	0.78

A comparable study investigated the impact of different times (3 minutes: fresh cement and 1 hour and 15 hours for pre-set cements) on the release behavior of pre-set brushite cement loaded with simvastatin drug (Mestres et al., 2016). The Korsmeyer–Peppas model was used to stimulate the drug release kinetics. The diffusional exponent revealed that the mechanism governing the drug release was anomalous. A good fit of the release profile to the model was found for the 1 h-set cement. The results revealed that the simvastatin release from the 3 min and the 1h set cements demonstrated a burst release phenomenon during the first 8 h and a

slower release for the next 4 days. The cement dried for 15h on the other hand, provided a prolonged release throughout the incubation time. Fitting parameters suggested that the simvastatin release mechanism was anomalous, with the corresponding n value of 0.77 for the 15h cement.

3.4. Post-release characterization of cements and ciprofloxacin

After the release test, the cement blocks immersed in the PBS solution for 18 days were recovered and dried at 37°C, then characterized by XRD, FTIR, and SEM to evaluate their physicochemical properties in terms of composition, morphology, and porosity. Dried and fresh composite cements loaded with 3 wt% ciprofloxacin, were chosen as representative samples for this study.

- **X-Ray Diffraction and Infrared Spectroscopy analyses**

Figure 14 compares the X-ray diffraction patterns of pre-and post-release cements (RCC-Cip3-D and RCC-Cip3-F) to the X-ray pattern of bone. A comparison of the diffractograms of the RCC-Cip3-D cements before and after 18 days of release revealed an evolution of the chemical composition of the cements towards a majority phase consisting of a low crystallinity apatite, analogous to the mineral composition of the bone, whose peaks were indexed according to the corresponding data of the JCPDS (No. 09-432). These diagrams also showed the presence of vaterite in trace form, as evidenced by the presence of two low-intensity vaterite peaks at 25.2° and 27.2° on the X-ray diagrams of RCC-Cip3-D cements attesting to the dissolution of a large amount of the vaterite after 18 days of incubation in PBS.

In the case of fresh cement (freeze-dried after 2 hours of its preparation), the diffractogram of RCC-Cip3-F cement before the release test indicated the presence of peaks characteristic of brushite, the most intense of which was located at 12°, and those typical of vaterite located at 21°, 25.2°, 27.2°, and 32.4°. Moreover, the diffractograms also showed the characteristic peaks of the newly formed apatite, which were mainly located at 26° and 32.2°. After release (immersion of the cement in PBS for 18 days) the composition of the cement evolved towards a low crystallinity apatite as the majority phase. In addition, the diffractogram of the RCC-Cip3-F cement revealed the presence of very weak peaks located at 25.2° and 27.2° typical of residual vaterite attesting those traces of vaterite remain in the cement matrix after release.

Furthermore, the results attested to the dissolution of the vaterite during the test which is accompanied by an increase in the intensity of the characteristic apatite peaks attesting that the Ca ions of the vaterite as well as the phosphate ions coming from the glass and also from the

PBS participated in the formation of the apatite within the cement during the dissolution/release test.

In conclusion, the diffractograms of RCC-Cip3-D and RCC-Cip3-F cements after release appeared to be similar indicating a composition consisting mainly of low crystallinity apatite which was similar to the mineral phase of bone tissue.

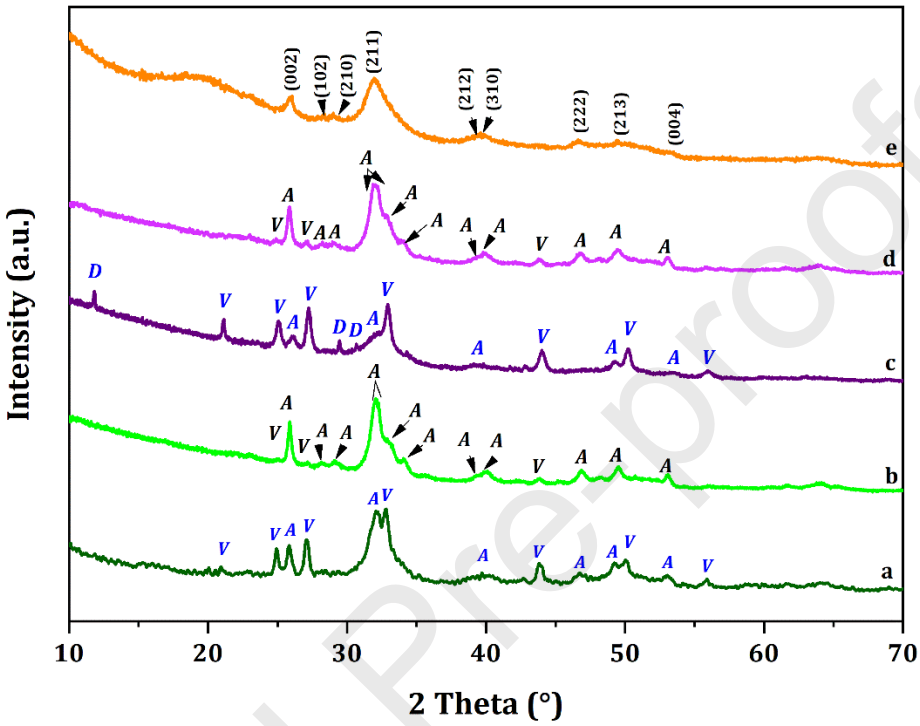

Figure 14. Pre- and post-release X-ray diagrams of RCC-Cip3-D (a: Pre-release and b: Post-release) and RCC-Cip3-F (c: Pre-release and d: post-release) cements, compared to the X-ray diagram of bone (e).

Figure 15 shows the infrared absorption spectra before and after release of RCC-Cip3-D and RCC-Cip3-F cements compared to the infrared spectrum of nano-carbonate apatite. The spectra of the cements analyzed after the release test RCC-Cip3-D (Figure 15b) and RCC-Cip3-F (Figure 15d) showed a significant decrease in the intensity of the vaterite bands particularly those located between 1420 - 1540 cm^{-1}. This decrease was due to the dissolution of the vaterite during the release test. The spectra of the cements after release were comparable with the spectrum of ANC which revealed phosphate bands typical of apatitic environments as well as bands attributable to vibrations of C-O carbonate bonds around 866 - 880 cm^{-1} (ν_2CO_3) and 1420 - 1540 cm^{-1} (ν_3CO_3).

Journal Pre-proofs

This analysis highlighted the disappearance of the bands located at 1262 cm^{-1} (C-N) and 1304 cm^{-1} (ν COOH + δC-OH) characteristic of ciprofloxacin, after release, indicating its elution from the cement matrix as confirmed by the release study.

The XRD and FTIR analyses were in agreement and attested to vaterite dissolution after 18 days of release for both dry and fresh cements. The post-release cements had a structure and composition comparable to that of the mineral part of the bone tissue.

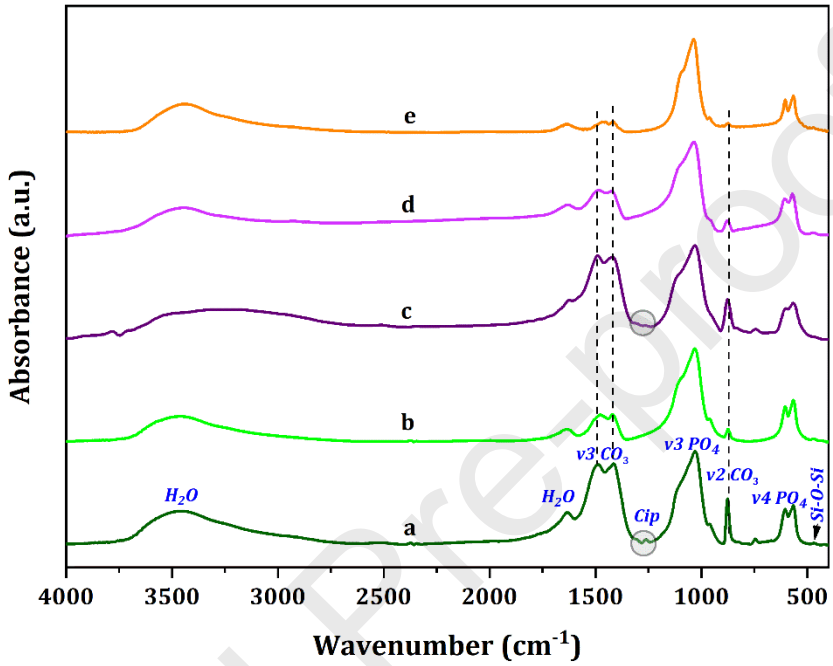

Figure 15. Pre- and post-release IR spectra of RCC-Cip3-D (a: Pre-release and b: Post-release) and RCC-Cip3-F (c: Pre-release and d: post-release) cements, compared to the X-ray pattern of carbonated nanocrystalline apatite (e: CNA).

- **Morphology and texture**

The results of the surface morphology evaluation of dried and fresh cements before and after release (RCC-Cip3-D et RCC-Cip9-D) are shown in Figure 16. The structure of all composite cements obtained after the release test became porous with the presence of macro and micropores of irregular size. The images showed blocks typical of the presence of bioactive glass (pink arrow), as well as the presence of the apatite phase (orange arrow) in the form of agglomerated crystals (fine needles). An apatite layer surrounding the bioactive glass was also observed in the SEM images. The presence of micrometer-sized pores was an imprint of the dissolution of the vaterite thus leaving pores with a size between 2 and 5 µm.

Journal Pre-proofs

Porosity, in particular, is one of the main parameters that affect the mechanical behavior and biological activity of CPCs. While porosity has a negative effect on the strength of the material, it allows for the growth of bone and blood vessels, thereby enhancing cement remodeling.

The presence of microporosity in the cements is useful for the circulation of biological fluids thus increasing the surface area of the CPC available for reaction with bone (Espanol et al., 2009). In addition, the existence of macroporosity in engineered cements will allow for the growth of blood vessels, thus accelerating the remodeling and replacement of implanted cements by bone.

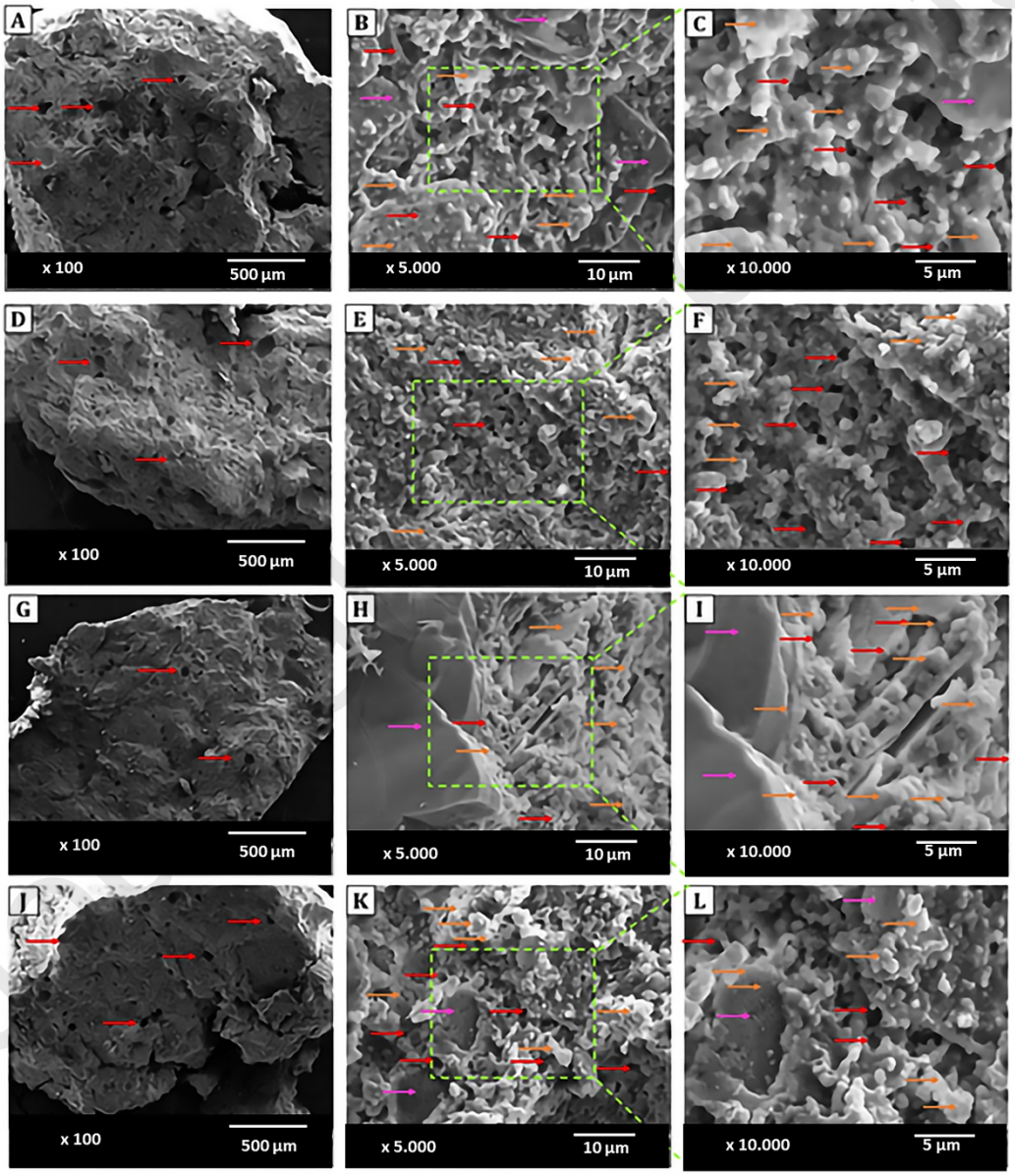

Figure 16. SEM images of cements after release RCC-Cip3-D (A, B, C) and RCC-Cip3-F (D, E, F) and RCC-Cip9-D (G, H, I) and RCC-Cip9-F (J, K, L). Red arrows (Pores), pink arrows (BG), and orange arrows (Apatite).

- **Ciprofloxacin stability**

The incorporation of drugs into calcium phosphate cements during the manufacturing process could influence their stability and could be modified and degraded. Thus, the evaluation of drug stability is an important study to determine if the molecules retain their integration and do not degrade during the setting and hardening of the cements. However, many studies have focused on the stability of biomolecules after bone cement formulation and also their stability in biological fluids.

In this work, to evaluate the stability of the ciprofloxacin molecule, the pure ciprofloxacin (15/mg/L) and the ciprofloxacin solution collected from the release medium (after 18 days of the release test) were analyzed using HPLC-MS analysis.

The obtained results (figure 17) reveal that the HPLC chromatogram of the sample collected from the release medium after 18 days is similar to that of pure ciprofloxacin and no degradation products of the ciprofloxacin molecule were detected after 18 days of release. This result indicates that this molecule has maintained its stability during formulation, setting, and hardening of the cement, as well as during the release test.

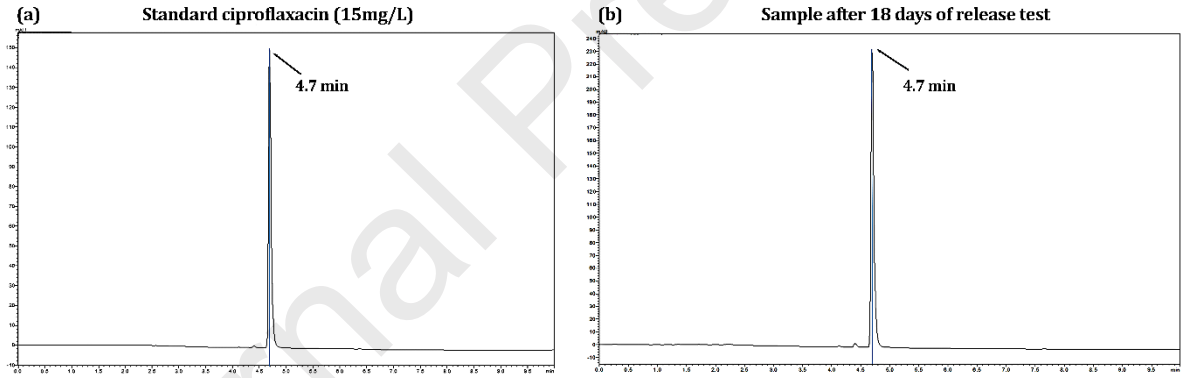

Figure 17. HPLC Chromatograms of (a) ciprofloxacin standard (15 mg/L) and (b) ciprofloxacin solution (23 mg/L) collected after 18 days of release.

3.5. Evaluation of antibacterial activity

The antibacterial activity of the prepared cements against Staphylococcus aureus (S. aureus) and Escherichia coli (E. coli) was examined qualitatively by the agar diffusion method. RCC, RCC-Cip3-D, and RCC-Cip9-D cements were tested to evaluate the effect of ciprofloxacin doses on antibacterial activity (figure 18). Antibacterial activity was assessed by calculating the diameter of the zone of inhibition. Table 7 summarizes the results of the inhibition zone diameter measurements.

Journal Pre-proofs

The results showed that the antibiotic-free cement (RCC) had no antibacterial activity against *S. aureus* and *E. coli* strains (no inhibition zone was observed around this compound). Ciprofloxacin-containing cements significantly inhibited the growth of these bacteria around the discs, whether for *S. aureus* or *E. coli*. The incorporation of 3 wt% ciprofloxacin in the composite cement (RCC-Cip3-D) resulted in a zone of inhibition diameter of 15.5 mm and 14.5 mm for S. aureus and E. coli, respectively, attesting to its effectiveness in inhibiting the growth of these germs. Furthermore, it should be noted that increasing the dose of ciprofloxacin led to a slightly larger inhibition zone diameter reaching a value of 18.5 mm and 17.5 mm for S. aureus and E. coli, respectively. This increase in the zone of inhibition in the case of RCC-Cip9-D cement is attributed to the difference in the amounts of antibiotic released from the formulations examined as confirmed by the release study, showing that the diameter of the zone of inhibition was directly proportional to the amount of antibiotic released. The amounts of antibiotic released per day were at a therapeutic level and were close to the minimum inhibitory concentration (MIC) of ciprofloxacin which is in the range of 0.25 to 2 µg/ml (Raj et al., 2013), revealing the effectiveness of the formulated composites to inhibit the growth of *Staphylococcus aureus* and *Escherichia coli*, pathogens responsible for bone infection.

Similar findings were reported by Ait said et al., (Ait Said et al., 2021), which evaluated the antibacterial activity of hydroxyapatite-chitosan composites loaded with ciprofloxacin (HA-CS-CIP) against the bacteria *Staphylococcus aureus* and *Escherichia coli*. The results obtained indicate that the diameters of the zones of inhibition measured for the materials associated with ciprofloxacin are largely superior compared to the reference compounds (HA, CS and HA-CS). A similar trend was also reported by Chandrasekar et al. who demonstrate that increasing the concentration of the antibiotic nisin increases the diameter of the zone of inhibition (Chandrasekar et al., 2015). The microbiological tests performed in this work show that the doses incorporated in the solid phase of the cements inhibited the growth of *S. aureus* and *E. coli* strains attesting to the possibility of conferring antibacterial properties to the tested cements.

Journal Pre-proofs

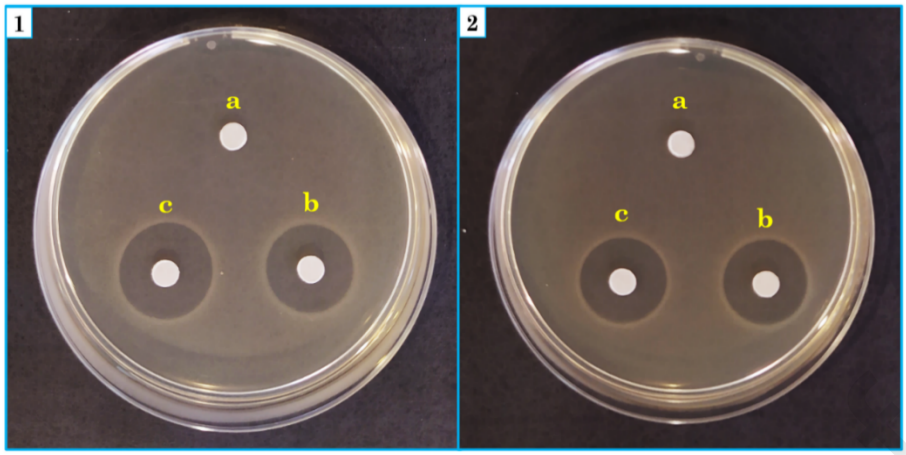

Figure 18. Antibacterial activity of RCC (a), RCC-Cip3-D (b), and RCC-Cip9-D (c) composite cements against *Escherichia coli* (1) and *Staphylococcus aureus* (2) bacteria.

Table 7. Inhibition zones diameters of RCC (reference), RCC-Cip3-D, and RCC-Cip9-D composite cements against Staphylococcus aureus (S. aureus) and Escherichia coli (E. coli) bacteria.

Cement	**Inhibition zone diameter (mm)**	
	S. aureus	***E. coli***
RCC	ND*	ND*
RCC-Cip3-D	15.5	14.5
RCC-Cip9-D	18.5	17.5

ND*: Not detected

Journal Pre-proofs

4. Conclusions

In the present work, we report a promising pathway for developing an injectable and antibacterial composite cement by incorporating ciprofloxacin antibiotic into the powder phase of the cement RCC. We demonstrated that the cements loaded with 3 and 9% ciprofloxacin exhibit appropriate characteristics in terms of the desired properties for clinical applications, such as a rapid setting reaction, a setting time of approximately 17 minutes for RCC-Cip9, an excellent injectability (95%), good cohesion and a compressive strength exceeding 8 MPa, which is comparable of that of the spongy bone.

This study demonstrated that the dry and fresh cements exhibited sustained release profiles over 18 days, with the elution rate controlled by the incorporated dose of ciprofloxacin as well as the state of the cements. The modeling of release data with Korsmeyer - Peppas indicated that the release process is mainly governed by a Fickian diffusion mechanism for dried cements. Furthermore, the findings revealed that the release behavior was affected by the antibiotic concentration and the cement state. The amounts of antibiotic released per day were at a therapeutic level revealing the efficiency of the formulated composites to inhibit the growth of *Staphylococcus aureus* and *Escherichia coli* bacteria.

The composite cements RCC and RCC-Cip appear as promising candidates as a substitute for mini-invasive surgery and drug delivery system. Further research, particularly on the biological response, is required to validate the clinical utility.

Acknowledgments

This work was supported by the OCP Foundation (Morocco) through the APPHOS Program (project ID: MAT-BAR-01/2017). The authors further thank the Center of Analysis and Characterization Center (CAC) of Cadi Ayyad University. We would like also to thank especially Pr. Rachid HAKKOU for Mechanical properties, Pr. Mansour SOBEH, and Mr. Badreddine DRISSI from AGBS-AGROBIOSCIENCES (UM6P) for HPLC-MS analysis.

Journal Pre-proofs

References

Ait Said, H., Noukrati, H., Oudadesse, H., Ben Youcef, H., Lefeuvre, B., Hakkou, R., Lahcini, M., Barroug, A., 2021. Formulation and characterization of hydroxyapatite-based composite with enhanced compressive strength and controlled antibiotic release. J. Biomed. Mater. Res. - Part A. https://doi.org/10.1002/jbm.a.37186

Alexopoulou, M., Mystiridou, E., Mouzakis, D., Zaoutsos, S., Fatouros, D.G., Bouropoulos, N., 2016. Preparation, characterization and in vitro assessment of ibuprofen loaded calcium phosphate/gypsum bone cements. Cryst. Res. Technol. 51, 41–48.

Alkhraisat, M.H., Rueda, C., Cabrejos-Azama, J., Lucas-Aparicio, J., Mariño, F.T., Torres García-Denche, J., Jerez, L.B., Gbureck, U., Cabarcos, E.L., 2010. Loading and release of doxycycline hyclate from strontium-substituted calcium phosphate cement. Acta Biomater. 6, 1522–1528. https://doi.org/10.1016/j.actbio.2009.10.043

Bazán Henostroza, M.A., Diniz Tavares, G., Nishitani Yukuyama, M., De Souza, A., José Barbosa, E., Carlos Avino, V., dos Santos Neto, E., Rebello Lourenço, F., Löbenberg, R., Araci Bou-Chacra, N., 2022. Antibiotic-loaded lipid-based nanocarrier: A promising strategy to overcome bacterial infection. Int. J. Pharm. 621. https://doi.org/10.1016/j.ijpharm.2022.121782

Beck-Broichsitter, B.E., Smeets, R., Heiland, M., 2015. Current concepts in pathogenesis of acute and chronic osteomyelitis. Curr. Opin. Infect. Dis. 28, 240–245. https://doi.org/10.1097/QCO.0000000000000155

Bu, D., Zhou, Y., Yang, C., Feng, H., Cheng, C., Zhang, M., Xu, Z., Xiao, L., Liu, Y., Jin, Z., 2021. Preparation of quaternarized N-halamine-grafted graphene oxide nanocomposites and synergetic antibacterial properties. Chinese Chem. Lett. 32, 3509–3513. https://doi.org/10.1016/j.cclet.2021.03.007

Canal, C., Pastorino, D., Mestres, G., Schuler, P., Ginebra, M.P., 2013a. Relevance of microstructure for the early antibiotic release of fresh and pre-set calcium phosphate cements. Acta Biomater. 9, 8403–8412. https://doi.org/10.1016/j.actbio.2013.05.016

Canal, C., Pastorino, D., Mestres, G., Schuler, P., Ginebra, M.P., 2013b. Relevance of microstructure for the early antibiotic release of fresh and pre-set calcium phosphate cements. Acta Biomater. 9, 8403–8412. https://doi.org/10.1016/j.actbio.2013.05.016

Chandrasekar, V., Knabel, S.J., Anantheswaran, R.C., 2015. Modeling development of inhibition zones in an agar diffusion bioassay. Food Sci. Nutr. 3, 394–403. https://doi.org/10.1002/fsn3.232

Daley, E., Kurdziel, M.D., Koueiter, D., Moore, D.D., 2018. Characterization of doxycycline-loaded calcium phosphate cement: implications for treatment of aneurysmal bone cysts. J. Mater. Sci. Mater. Med. 29. https://doi.org/10.1007/s10856-018-6117-6

Espanol, M., Perez, R.A., Montufar, E.B., Marichal, C., Sacco, A., Ginebra, M.P., 2009. Intrinsic porosity of calcium phosphate cements and its significance for drug delivery and tissue engineering applications. Acta Biomater 5, 2752–2762. https://doi.org/10.1016/j.actbio.2009.03.011

Fosca, M., Rau, J. V., Uskoković, V., 2022. Factors influencing the drug release from calcium phosphate cements. Bioact. Mater. 7, 341–363. https://doi.org/10.1016/j.bioactmat.2021.05.032

Ghosh, S., Wu, V., Pernal, S., Uskoković, V., 2016. Self-Setting Calcium Phosphate Cements with Tunable Antibiotic Release Rates for Advanced Antimicrobial Applications. ACS Appl. Mater. Interfaces 8, 7691–7708. https://doi.org/10.1021/acsami.6b01160

Ginebra, M.-P., Montufar, E.B., 2019. Cements as bone repair materials, Second Edi. ed, Bone Repair Biomaterials. Elsevier Ltd. https://doi.org/10.1016/b978-0-08-102451-5.00009-3

Ginebra, M.P., Canal, C., Espanol, M., Pastorino, D., Montufar, E.B., 2012a. Calcium phosphate cements as drug delivery materials. Adv. Drug Deliv. Rev. 64, 1090–1110.

https://doi.org/10.1016/j.addr.2012.01.008
Ginebra, M.P., Canal, C., Espanol, M., Pastorino, D., Montufar, E.B., 2012b. Calcium phosphate cements as drug delivery materials. Adv. Drug Deliv. Rev. 64, 1090–1110. https://doi.org/10.1016/j.addr.2012.01.008
Hamanishi, C., Kitamoto, K., Tanaka, S., Otsuka, M., Doi, Y., Kitahashi, T., 1996. A self-setting TTCP-DCPD apatite cement for release of vancomycin. J. Biomed. Mater. Res. 33, 139–143. https://doi.org/10.1002/(SICI)1097-4636(199623)33:3<139::AID-JBM3>3.0.CO;2-R
Hesaraki, S., Nemati, R., 2009. Cephalexin-loaded injectable macroporous calcium phosphate bone cement. J. Biomed. Mater. Res. - Part B Appl. Biomater. 89, 342–352. https://doi.org/10.1002/jbm.b.31222
Jenkins, A., An Diep, B., Mai, T.T., Vo, N.H., Warrener, P., Suzich, J., Kendall Stover, C., Sellman, B.R., 2015. Differential expression and roles of Staphylococcus aureus virulence determinants during colonization and disease. MBio 6. https://doi.org/10.1128/mBio.02272-14
Jindong, Z., Hai, T., Junchao, G., Bo, W., Li, B., Qiang, W.B., 2010. Evaluation of a novel osteoporotic drug delivery system in vitro: alendronate-loaded calcium phosphate cement. Orthopedics 33.
Kai, M., Zhang, W., Xie, H., Liu, L., Huang, S., Li, X., Zhang, Z., Liu, Y., Zhang, B., Song, J., Wang, R., 2018. Effects of linker amino acids on the potency and selectivity of dimeric antimicrobial peptides. Chinese Chem. Lett. 29, 1163–1166. https://doi.org/10.1016/j.cclet.2018.04.011
Kisanuki, O., Yajima, H., Umeda, T., Takakura, Y., 2007. Experimental study of calcium phosphate cement impregnated with dideoxy-kanamycin B. J. Orthop. Sci. 12, 281–288. https://doi.org/10.1007/s00776-007-1124-3
Li, L., Ma, W., Cheng, X., Ren, X., Xie, Z., Liang, J., 2016. Synthesis and characterization of biocompatible antimicrobial N-halamine-functionalized titanium dioxide core-shell nanoparticles. Colloids Surfaces B Biointerfaces 148, 511–517. https://doi.org/10.1016/j.colsurfb.2016.09.030
Mabrouk, M., Mostafa, A.A., Oudadesse, H., Mahmoud, A.A., El-Gohary, M.I., 2013. Bioactivity and drug delivering ability of a chitosan/46S6 melted bioactive glass biocomposite scaffold. InterCeram Int. Ceram. Rev. 62, 444–452.
Mabroum, H., Noukrati, H., Ben, H., Oudadesse, H., Barroug, A., 2022. The effect of bioactive glass particle size and liquid phase on the physical-chemical and mechanical properties of carbonated apatite cement. Ceram. Int. https://doi.org/10.1016/j.ceramint.2022.06.126
Mabroum, H., Noukrati, H., Ben youcef, H., Lefeuvre, B., Oudadesse, H., Barroug, A., 2021. Physicochemical, setting, rheological, and mechanical properties of a novel bio-composite based on apatite cement, bioactive glass, and alginate hydrogel. Ceram. Int. https://doi.org/10.1016/j.ceramint.2021.05.106
Mestres, G., Kugiejko, K., Pastorino, D., Unosson, J., Ohman, C., Karlsson Ott, M., Ginebra, M.P., Persson, C., 2016. Changes in the drug release pattern of fresh and set simvastatin-loaded brushite cement. Mater Sci Eng C Mater Biol Appl 58, 88–96. https://doi.org/10.1016/j.msec.2015.08.016
Mircioiu, C., Voicu, V., Anuta, V., Tudose, A., Celia, C., Paolino, D., Fresta, M., Sandulovici, R., Mircioiu, I., 2019. Mathematical modeling of release kinetics from supramolecular drug delivery systems. Pharmaceutics 11, 1–45. https://doi.org/10.3390/pharmaceutics11030140
Montazerolghaem, M., Karlsson Ott, M., 2014. Sustained release of simvastatin from premixed injectable calcium phosphate cement. J. Biomed. Mater. Res. - Part A 102, 340–347. https://doi.org/10.1002/jbm.a.34702

Nadig, N.S., Shaw, K.A., Parada, S.A., 2020. Exploring Penicillin G as an Intrawound Antibiotic Powder for Prevention of Postoperative Shoulder Infections: Does It Exhibit In Vitro Chondrotoxicity? J. Orthop. Res. 38, 726–730. https://doi.org/10.1002/jor.24524

Nandi, S.K., Bandyopadhyay, S., Das, P., Samanta, I., Mukherjee, P., Roy, S., Kundu, B., 2016. Understanding osteomyelitis and its treatment through local drug delivery system. Biotechnol. Adv. 34, 1305–1317. https://doi.org/10.1016/j.biotechadv.2016.09.005

Noukrati, H., Cazalbou, S., Demnati, I., Rey, C., Barroug, A., Combes, C., 2016. Injectability, microstructure and release properties of sodium fusidate-loaded apatitic cement as a local drug-delivery system. Mater. Sci. Eng. C 59, 177–184. https://doi.org/10.1016/j.msec.2015.09.070

Pachaiappan, R., Rajendran, S., Show, P.L., Manavalan, K., Naushad, M., 2021. Metal/metal oxide nanocomposites for bactericidal effect: A review. Chemosphere 272, 128607. https://doi.org/10.1016/j.chemosphere.2020.128607

Pastorino, D., Canal, C., Ginebra, M.P., 2015a. Drug delivery from injectable calcium phosphate foams by tailoring the macroporosity-drug interaction. Acta Biomater 12, 250–259. https://doi.org/10.1016/j.actbio.2014.10.031

Pastorino, D., Canal, C., Ginebra, M.P., 2015b. Multiple characterization study on porosity and pore structure of calcium phosphate cements. Acta Biomater 28, 205–214. https://doi.org/10.1016/j.actbio.2015.09.017

Raj, M.S., Arkin, V.H., Jagannath, M., 2013. Nanocomposites based on polymer and hydroxyapatite for drug delivery application. Indian J. Sci. Technol. 6, 4653–4658.

Ranjkesh, B., Chevallier, J., Salehi, H., Cuisinier, F., Isidor, F., Løvschall, H., Løvschall, H., 2016. Apatite precipitation on a novel fast-setting calcium silicate cement containing fluoride 7931. https://doi.org/10.1080/23337931.2016.1178583

Rao, N., Ziran, B.H., Lipsky, B.A., 2011. Treating osteomyelitis: Antibiotics and surgery. Plast. Reconstr. Surg. 127, 177–187. https://doi.org/10.1097/PRS.0b013e3182001f0f

Ratier, A., Freche, M., Lacout, J.L., Rodriguez, F., 2004. Behaviour of an injectable calcium phosphate cement with added tetracycline. Int. J. Pharm. 274, 261–268. https://doi.org/10.1016/j.ijpharm.2004.01.021

Ratier, A., Gibson, I.R., Best, S.M., Freche, M., Lacout, J.L., Rodriguez, F., 2001. Setting characteristics and mechanical behaviour of a calcium phosphate bone cement containing tetracycline. Biomaterials 22, 897–901. https://doi.org/10.1016/S0142-9612(00)00252-0

Shah, F.A., Brauer, D.S., Hill, R.G., Hing, K.A., 2015. Apatite formation of bioactive glasses is enhanced by low additions of fl uoride but delayed in the presence of serum proteins. Mater. Lett. 153, 143–147. https://doi.org/10.1016/j.matlet.2015.04.013

Takechi, M., Miyamoto, Y., Momota, Y., Yuasa, T., Tatehara, S., Nagayama, M., Ishikawa, K., Suzuki, K., 2002. The in vitro antibiotic release from anti-washout apatite cement using chitosan. J. Mater. Sci. Mater. Med. 13, 973–978. https://doi.org/10.1023/A:1019816830793

Uskoković, V., 2019. Mechanism of formation governs the mechanism of release of antibiotics from calcium phosphate nanopowders and cements in a drug-dependent manner. J. Mater. Chem. B 7, 3982–3992. https://doi.org/10.1039/c9tb00444k

Verron, E., Pissonnier, M.L., Lesoeur, J., Schnitzler, V., Fellah, B.H., Pascal-Moussellard, H., Pilet, P., Gauthier, O., Bouler, J.M., 2014. Vertebroplasty using bisphosphonate-loaded calcium phosphate cement in a standardized vertebral body bone defect in an osteoporotic sheep model. Acta Biomater 10, 4887–4895. https://doi.org/10.1016/j.actbio.2014.07.012

Wang, Q., Ge, L., Wang, L., Xu, Y., Miao, S., Yu, G., Shen, Y., 2021. Formulation optimization and in vitro antibacterial ability investigation of azithromycin loaded FDKP microspheres dry powder inhalation. Chinese Chem. Lett. 32, 1071–1076. https://doi.org/10.1016/j.cclet.2020.03.062

Wu, S., Lei, L., Bao, C., Liu, Jin, Weir, M.D., Ren, K., Schneider, A., Oates, T.W., Liu, Jun, Xu, H.H.K., 2021. An injectable and antibacterial calcium phosphate scaffold inhibiting Staphylococcus aureus and supporting stem cells for bone regeneration. Mater. Sci. Eng. C 120. https://doi.org/10.1016/j.msec.2020.111688

Wu, S., Liu, Y., Lei, L., Zhang, H., 2019. Antisense yycG Regulation of Antibiotic Sensitivity of Methicillin-Resistant Staphylococcus aureus in Chronic Osteomyelitis. Surg. Infect. (Larchmt). 20, 472–479. https://doi.org/10.1089/sur.2019.016

Yang, Z., Hao, X., Chen, S., Ma, Z., Wang, W., Wang, C., Yue, L., Sun, H., Shao, Q., Murugadoss, V., Guo, Z., 2019. Long-term antibacterial stable reduced graphene oxide nanocomposites loaded with cuprous oxide nanoparticles. J. Colloid Interface Sci. 533, 13–23. https://doi.org/10.1016/j.jcis.2018.08.053

Yousefi, A.M., 2019. A review of calcium phosphate cements and acrylic bone cements as injectable materials for bone repair and implant fixation. J. Appl. Biomater. Funct. Mater. 17. https://doi.org/10.1177/2280800019872594

Author Statement

Hanaa Mabroum: Investigation, validation, Formal analysis, Visualization, Writing- Original draft. **Hassan Noukrati**: Conceptualization, Methodology, Supervision, Writing - Reviewing and Editing, Funding acquisition. **Hamza EL BAZA:** Formal analysis, Investigation. **Hicham Ben Youcef**: Methodology, Reviewing, and Editing. **Hassane Oudadesse**: Supervision, Reviewing, and Editing. **Allal Barroug:** Supervision, Methodology, Reviewing and Editing, Funding acquisition, Project administration. All authors have read and agreed to the published version of the manuscript.

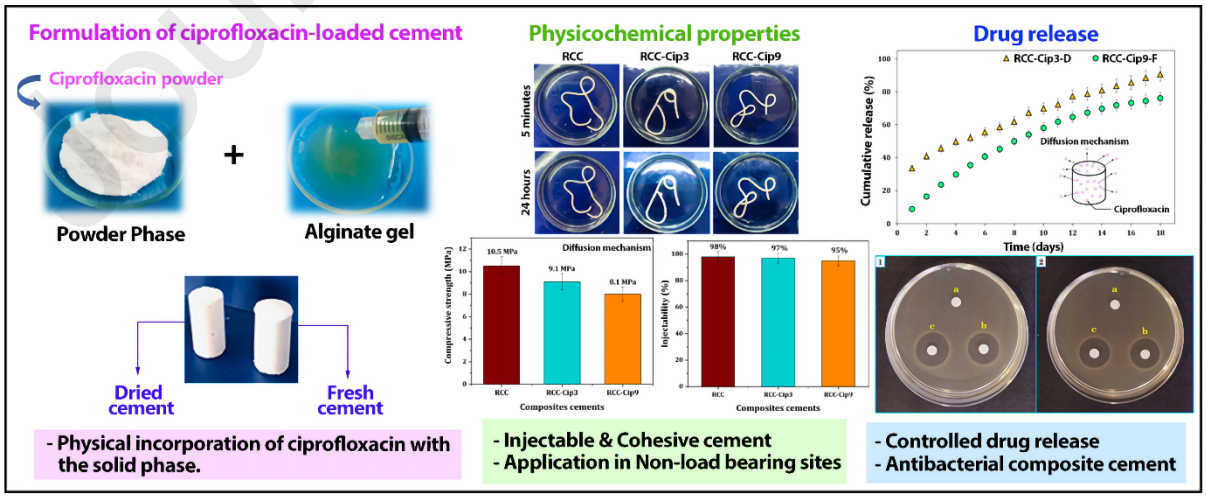

Journal Pre-proofs

Declaration of interests

☒ The authors declare that they have no known competing financial interests or personal relationships that could have appeared to influence the work reported in this paper.

☐ The authors declare the following financial interests/personal relationships which may be considered as potential competing interests:

Declaration of interests

☒ The authors declare that they have no known competing financial interests or personal relationships that could have appeared to influence the work reported in this paper.

☐ The authors declare the following financial interests/personal relationships which may be considered as potential competing interests:

Journal Pre-proofs